

**BEHAVIOUR AND STRENGTH OF RC COLUMNS RETROFITTED WITH
STEEL ANGLES AND STRIPS UNDER ECCENTRIC AXIAL LOADS**

DEBASISH SEN

MASTER OF SCIENCE IN ENGINEERING

(CIVIL & STRUCTURAL)



**DEPARTMENT OF CIVIL ENGINEERING
BANGLADESH UNIVERSITY OF ENGINEERING AND TECHNOLOGY
DHAKA, BANGLADESH**

MARCH 2017

**BEHAVIOUR AND STRENGTH OF RC COLUMNS RETROFITTED WITH
STEEL ANGLES AND STRIPS UNDER ECCENTRIC AXIAL LOADS**

DEBASISH SEN

A thesis submitted to the Department of Civil Engineering of Bangladesh University of Engineering and Technology, Dhaka in partial fulfillment of the requirement of the degree

of

MASTER OF SCIENCE IN ENGINEERING

(CIVIL & STRUCTURAL)



**DEPARTMENT OF CIVIL ENGINEERING
BANGLADESH UNIVERSITY OF ENGINEERING AND TECHNOLOGY
DHAKA, BANGLADESH**

MARCH 2017

CERTIFICATE OF APPROVAL

The thesis titled “**Behaviour and Strength of RC Columns Retrofitted with Steel Angles and Strips under Eccentric Axial Loads**” submitted by Debasish Sen, Student Number 0412042362P, Session April, 2012 has been accepted as satisfactory in partial fulfillment of the requirement for the degree of Master of Science in Engineering (Civil and Structural) on 25th March, 2017.

BOARD OF EXAMINERS

1. 

Dr. Mahbuba Begum **Chairman**
(Supervisor)
Professor
Department of Civil Engineering
BUET, Dhaka-1000
2. 

Dr. Abdul Muqtadir **Member**
(Ex-Officio)
Professor and Head
Department of Civil Engineering
BUET, Dhaka-1000
3. 

Dr. Raquib Ahsan **Member**
Professor
Department of Civil Engineering
BUET, Dhaka-1000
4. 

Dr. Md. Mozammel Hoque **Member**
(External)
Professor
Department of Civil Engineering
DUET, Gazipur

Declaration

Except for the contents where specific references have been made to the work of others, the studies embodied in this dissertation are the outcome of the research conducted by the author. No part of this dissertation has been submitted to any other University or other educational establishment for a Degree, Diploma or other qualification (except for publication).



Debasish Sen

Dedicated
To
My Beloved Parents

ACKNOWLEDGEMENT

The Author sincerely expresses his deepest gratitude to the Almighty.

The author would like to express sincere gratitude to Dr. Mahbuba Begum for the guidance, inspiration, and numerous hours spent to help in this research work. Her contribution as a supervisor and guide is truly appreciable. She was also gracious enough in giving sufficient leeway regarding the planning and execution of experimental work. Her valuable comments and insights helped to improve the work enormously. Her generosity and support will not be forgotten.

The author conveys deepest gratitude to his parents and family members for their unconditional inspiration and supports.

Finally, the author admits the supports of his colleagues especially Mr. Md. Mashfiqul Islam for his continuous inspiration.

ABSTRACT

This study intends to investigate the performance and behavior of steel jacketed Reinforced Concrete columns under eccentric loads. An experimental program has been designed to identify the behavior of jacketed RC columns under various levels of load eccentricity. This has been followed by a finite element based numerical simulation using constitutive material and appropriate contact modeling. In finite element model, both material and geometric nonlinearities were considered. The finite element models show fair agreement with the observed experimental results in terms of ultimate capacity and failure mode. This study also intends to investigate the performance of available analytical models to predict the capacity of steel angle and strip jacketed RC columns.

The results of this study indicate that steel angle and strip jacketing scheme performs well under both concentric and eccentric loading. The capacity enhancement has been found about 240% under concentric loads compared to un-strengthened RC column, whereas the capacity enhancement is relatively more under eccentric loading compared to concentric loading. However, for this particular case eccentricity reduces the ultimate capacity of steel cage jacketed RC column of about 15% when eccentricity to column width ratio changes from 0 to 0.45. It also changes the ductile behavior of jacketed RC columns. From the finite element analysis, it has been found that the mean of experimental to numerical ultimate load capacity ratio was about 0.95, which indicates a fair agreement with slight overestimation. On the other hand, the available analytical model can predict load-moment interaction curve of steel jacketed RC columns with a high level of safety margin.

TABLE OF CONTENT

ABSTRACT.....	vi
TABLE OF CONTENT.....	vii
LIST OF TABLES.....	xi
LIST OF FIGURES.....	xii
NOTATIONS.....	xv
CHAPTER 1 INTRODUCTION	1-4
1.1 General	1
1.2 Objective	2
1.3 Scope of the Study.....	2
1.4 Organization of Thesis	3
CHAPTER 2 LITERATURE REVIEW	5-25
2.1 Introduction	5
2.2 Theoretical Strength Restoring Mechanism.....	6
2.2.1 Concrete confinement.....	6
2.2.2 Composite action	7
2.3 Experimental Investigation	7
2.4 Numerical Investigation	13
2.5 Analytical Models	14
2.6 Comparative study of the Influence of Key Parameters	18
2.6.1 Grout material.....	18
2.6.2 Strip configuration.....	19
2.6.3 Angle size	20

2.6.4 Connection to specimen head	21
2.6.5 Eccentricity	22
2.6.6 Length of retrofitting	23
2.6.7 Load State during strengthening	23
2.7 Conclusions	24
CHAPTER 3 EXPERIMENTAL PROGRAM	26-36
3.1 General	26
3.2 Description of Test Specimens	26
3.3 Explanation of Test Parameter	27
3.4 Material Properties	28
3.4.1 Cement	28
3.4.2 Aggregate	28
3.4.3 Reinforcement	30
3.4.4 Steel angle and Strip	31
3.5 Test Column Fabrication	31
3.5.1 Concrete mix design	31
3.5.2 Concrete placement and curing	31
3.6 Strengthening of RC Columns	33
3.7 Instrumentation and Testing of Jacketed Column	33
CHAPTER 4 FINITE ELEMENT MODELLING	37-50
4.1 Introduction	37
4.2 Geometric Properties of the Finite Element Model	37
4.2.1 Element selection and mesh	37
4.2.2 Interaction of different components	39
4.2.3 End boundary conditions	41

4.3 Material Properties used in the Finite Element Model.....	41
4.3.1 Concrete damage plasticity model.....	41
4.3.2 Verification of concrete model.....	45
4.3.3 Material model of steel.....	46
4.4 Load Application and Solution Strategy.....	49
4.4.1 Application of load.....	49
4.4.2 Solution strategy.....	49
CHAPTER 5 RESULTS AND DISCUSSIONS.....	51-76
5.1 General.....	51
5.2 Experimental Results.....	52
5.2.1 Load deflection responses.....	52
5.2.2 Axial load capacity and displacement ductility.....	53
5.2.3 Failure modes.....	55
5.2.4 Load-Moment interaction of steel angles and strips jacketed RC column.....	62
5.3 Performance of Finite Element Model.....	63
5.3.1 Initial model verification.....	63
5.3.2 Efficiency of strengthening.....	65
5.3.3 Concrete confinement.....	65
5.3.4 Mid-height displacement of angle.....	69
5.4 Performance of Analytical Models.....	71
5.4.1 Compressive capacity prediction models.....	71
5.4.2 Failure envelope prediction model.....	73
5.5 Summary.....	75
CHAPTER 6 CONCLUSIONS AND RECOMMENDATIONS.....	77-79
6.1 General.....	77

6.2 Conclusions	78
6.3 Recommendations for Future Work	79
REFERENCES	80
APPENDIX	84

LIST OF TABLES

Table 2.1: Contribution of angles to ultimate load capacities.....	22
Table 2.2: Effect of length of angles on the ultimate load capacity.....	23
Table 3.1: Details of the test specimens.....	27
Table 3.2: Properties of aggregates.....	29
Table 3.3: Properties of steel elements of jacketed RC columns.....	29
Table 3.4: ACI concrete mix design at Saturated Surface Dry (SSD) condition.....	31
Table 5.1: Ultimate load capacities of test columns.....	54
Table 5.2: Ultimate load capacities of finite element models.....	63
Table 5.3: Efficiency of steel angle and strip jacketing method.....	65
Table 5.4: Predicted capacities from different analytical models.....	72
Table 5.5: Axial and moment capacity of jacketed column.....	75
Table A.1 Details of samples and results with different number of strips and eccentricity.....	84
Table A.2 Details of samples and results with different strip configuration.....	86

LIST OF FIGURES

Figure 2.1 Schematic diagram of steel angle and strip strengthened RC column (a) Elevation and (b) Cross section	6
Figure 2.2 Confinement due to steel cage (a) effective confinement in elevation, (b) confinement pressure distribution at strip level, and (c) effective confinement in plan (Redrawn from Nagaprasad <i>et al.</i> , 2009)	8
Figure 2.3 Schematic diagrams of loads on steel angle (Redrawn from Badalamenti <i>et al.</i> , 2010).....	9
Figure 2.4 Failure modes of jacketed columns with buckling of corner angle.....	9
Figure 2.5 Failure at un-strengthened part of partially jacketed columns	10
Figure 2.6 Failure of jacketed column by concrete splitting	10
Figure 2.7 Failure of jacketed column under eccentric loading.....	11
Figure 2.8 Confining pressure distributions at batten level (Redrawn from Campione, 2011).....	15
Figure 2.9 Effect of grout materials on the ultimate load capacity.....	19
Figure 2.10 Effect of (a) strip spacing and (b) strip thickness on the ultimate capacity	20
Figure 2.11 Effect of angle size on ultimate load capacity.....	21
Figure 2.12 Effect of angles and specimen head's connectivity on ultimate load capacity	21
Figure 2.13 Effect of eccentricity of loading on the ultimate load capacity.....	22
Figure 2.14 Effect of load state during strengthening on the ultimate load capacity	24
Figure 3.1 Typical steel angle and strip jacketed RC column	28
Figure 3.2 Gradation curve of fine aggregates.....	29
Figure 3.3 Load-deflection curve of (a) 10mm diameter reinforcement and (b) Steel angle	30
Figure 3.4 Concrete Placement of RC Column (a) Mechanical Mixture, (b) Fresh Concrete (c) Formworks (d) Slump test (e) Compaction and (f) Constructed RC columns	32
Figure 3.5 Steps of steel jacketing (a) Attachment of angle and (b) Welded Strips.....	33
Figure 3.6 Universal Testing Machine (UTM).....	34
Figure 3.7 Schematic diagram of column cap used for eccentric loading	34
Figure 3.8 Un-strengthened RC column before loading.....	35
Figure 3.9 Strengthened RC column before loading	35
Figure 3.10 Schematic diagram of test setup for pure bending test.....	36

Figure 3.11 Setup for pure bending test of strengthened RC member.....	36
Figure 4.1 Finite elements used (a) C3D8R and (b) T3D2.....	38
Figure 4.2 Mesh of steel angle and strip jacketed RC column	38
Figure 4.3 Qualitative shear stress vs. contact pressure relationship.....	40
Figure 4.4 Qualitative response of concrete to (a) Compression and (b) Tension	43
Figure 4.5 Compressive stress strain curve for concrete	44
Figure 4.6 Tensile stress strain curve for concrete	44
Figure 4.7 Finite element model of Concrete cylinder	45
Figure 4.8 Stress-strain curve of cylinder under compression.....	45
Figure 4.9 Qualitative stress strain curve of steel.....	46
Figure 4.10 Bilinear stress strain curve of Steel Angles.....	47
Figure 4.11 Bilinear stress strain curve of Steel Strips.....	47
Figure 4.12 Bilinear stress strain curve of 10mm diameter reinforcement.....	48
Figure 4.13 Bilinear stress strain curve of 8mm diameter reinforcement.....	48
Figure 4.14 Newton-Raphson solution strategy.....	50
Figure 5.1 Axial Load-Displacement curves of un-strengthened and strengthened RC columns	52
Figure 5.2 Axial Force-Displacement graphs of jacketed columns with different load eccentricity .	53
Figure 5.3 Effect of eccentricity on axial load capacity	55
Figure 5.4 Failure mode of un-strengthened RC column under concentric loads	56
Figure 5.5 Buckling of longitudinal reinforcements in un-strengthened RC column under concentric loads	56
Figure 5.6 (a) Top concrete crushing and (b) Bottom concrete crack of un-strengthened RC column under concentric loads	56
Figure 5.7 Steel angles buckling at (a) Top and (b) Bottom of strengthened RC column under concentric loads	57
Figure 5.8 Concrete splitting of strengthened RC column at bottom under concentric loads	57
Figure 5.9 Failure mode of strengthened RC column with eccentricity of 15mm	58
Figure 5.10 Buckling of steel angles and concrete crushing in between strips with eccentricity of 15mm	58
Figure 5.11 Failure mode of strengthened RC column with eccentricity of 37.5 mm	59

Figure 5.12 Buckling of steel angles and concrete spalling in between strips with an eccentricity of 37.5mm	59
Figure 5.13 Buckling of compression side steel angles at top with an eccentricity of 37.5 mm.....	60
Figure 5.14 Failure mode of strengthened RC column with an eccentricity of 67.5 mm.....	61
Figure 5.15 Buckling of steel angles and concrete crushing in between strips with eccentricity of 67.5mm	61
Figure 5.16 Failure modes (a) overall deflected shape and (b) shear crack of Steel jacketed RC column under pure bending	61
Figure 5.17 Interaction Diagram of RC column with and without jacketing	62
Figure 5.18 Deformed shape of the strengthened RC column with load eccentricity of 15 mm.....	64
Figure 5.19 Axial load carried by RC core for different eccentricities	66
Figure 5.20 Maximum Concrete stresses at ultimate load for the column with different eccentricities	67
Figure 5.21 Confined concrete stress of jacketed RC columns at ultimate capacity	68
Figure 5.22 Load carried by RC core of jacketed columns at ultimate capacity	68
Figure 5.23 Stress distributions at mid-height section for column having different load eccentricities	70
Figure 5.24 Effect of eccentricity on the mid height displacement	71
Figure 5.25 Normalized ultimate load capacities from different analytical models.....	73
Figure 5.26 Analytical Interaction Diagram of jacketed RC column	74

NOTATIONS

A_c	Area of concrete column
A_s	Area of steel angles
A_s/A_{sl}	Area of longitudinal reinforcement
b	Side dimensions of column
d	Width of column
d_c/d_t	Damage parameter
e	Eccentricity
E_c	Modulus of elasticity of concrete
E_h	Hardening modulus of steel angles
E_r	Reduced modulus
E_s/E_L	Modulus of elasticity of steel
$f_c/f_{co}/f_{cd}/f_{cu}$	Compressive strength of unconfined concrete
f_{cc}	Confined concrete strength
f_l	Confining pressure due to strips and angles
f_{ydb}	Yielding design stress of steel strip
f_{yl}/f_y	Yield stress of the steel plates
f_{ys}	Yield stress of reinforcement steel
L_1	Side of a steel angle
M_p	Plastic moment capacity of an angle
n	Dimension-less load carrying capacity of confined concrete core
n_a	Dimension-less maximum axial force available in directly loaded angles
N_c	Axial load carried by concrete
N_L	Axial load supported by the cage at the end of a strip
P_{ult}	Ultimate load capacity of strengthened column.
S/s	Spacing of steel strips
s_2/l_2	Width of steel strip
t_1	Thickness of steel angle
t_2	Thickness of steel strip

αL_1	Equivalent rectangular cross section side of angle
β	A material parameter depending on the shape of the stress- strain diagram
γ	Equivalent slip rate
μ	Frictional coefficient between concrete and steel
ε_c	Strain of concrete
$\varepsilon_c^{\sim in}$	Inelastic strain
$\varepsilon_c^{\sim pl}$	Plastic strain
ε_{nom}	Nominal strain of steel
ν_c	Poisson's coefficient of the concrete.
ρ_s	Ratio of steel battens in the area (b x S)
σ_{true}	True stress of steel
σ_{true}	Nominal stress of steel
τ	Equivalent shear stress
ω_s	Mechanical ratio of steel battens

1.1 General

Now-a-days retrofitting, repairing, and restoring are the important aspect for structural engineering community. Retrofitting can be done by using the approach of local strengthening of structural elements (i.e. beams, columns) or global strengthening of structure (i.e. insertion of bracing or shear wall). Columns are the most important elements of structural system to carry vertical load as well as to provide lateral resistance. Sometimes, columns have not enough strength due to inadequate shear reinforcements or splice length or bad construction workmanship. Column capacity can also be deteriorated by previous seismic action or fire. In these cases, columns have to be locally strengthened to ensure life safety using one of the following approaches, e.g. additional reinforced concrete layer, ferrocement jacketing, fiber reinforced polymer wrapping, steel jacketing etc. Among them steel jacketing is comparatively easy to install at site and also effective to increase load capacity. Steel jacketing consists of four angles attached with corners of column and discrete horizontal steel plates with a specific spacing which are welded to the angles. Horizontal steel plates are termed as strips or battens. The welding length should be sufficient to avoid shear failure at joints. In practice, total assembly is termed as steel cage. The gaps between installed steel cage and existing concrete surfaces are filled with cement grout or epoxy to ensure a continuous contact.

Several researchers conducted studies to evaluate the load carrying capacity of steel angle and strip strengthened Reinforced Concrete (RC) columns. Different key parameters have been incorporated in those researches, which have immense influences on the load carrying capacity and behavior. The main deficiency found in literature is the insufficient studies on the steel angle and strip strengthened RC columns subjected to eccentric loads. So, further studies are required on the behavior under eccentricities i.e. axial load and bending moment.

To meet this need, an experimental attempt has been taken to investigate the behavior of steel angle and strip jacketed RC columns under eccentric loading. The observed results have also been simulated with finite element models. This study also intends to verify existing capacity prediction models under concentric load and moment-load domain.

1.2 Objectives of the Study

The objectives of this study are as follows-

1. To conduct experimental investigations on RC columns strengthened with steel angles and strips under eccentric axial loads.
2. To develop the load-moment interaction diagram for steel jacketed RC columns.
3. To simulate the experimental work using Finite Element model.
4. To study the available analytical models for predicting the capacity of RC columns strengthened using steel angles and strips.

1.3 Scope of the Study

Initially, a rigorous review of the steel angle and strip jacketed RC columns has been done. From available experimental data in literature, a comparative study has been conducted to figure out the key parameters and their effects on the performance of steel angle and strip jacketed RC columns. Deficiency has been found in the area of researches on the load eccentricity, which has profound influences on the behavior of jacketed RC columns. This comparative study has invoked to investigate the effect of load eccentricity.

This study is mainly focused to investigate the behaviour of steel angle and strip jacketed RC columns under eccentric load. To implement this objective, an experimental program has been designed with one un-strengthened and five strengthened RC columns. The RC columns have 150 mm square cross section, 1.4% longitudinal reinforcement and a

slenderness ratio of 10. Strengthened columns have been jacketed with steel angles (8.4% of concrete cross section) and strips. The main variance parameter is the load eccentricity of columns. The effect of load eccentricity has been investigated experimentally in terms of load-deflection curve, ultimate capacity and displacement ductility.

Further effort has been given to simulate the experimental works in Finite Element (FE) platform (ABAQUS/Standard). Numerical simulation has been conducted by considering non-linear and bi-linear behaviour of concrete and steel respectively. Comparisons have been made between experimental and numerical models in terms of ultimate load capacities and failure modes. FEM models show fair agreement with the experimental results. After that, FE models have been utilized to investigate the effect of load eccentricity on the concrete confinement, mid-height displacement of strengthened RC column and stresses on angles at failure etc. numerically.

Endeavor has also been given to develop a load-moment interaction diagram from experimental data. Validation of available analytical model regarding axial capacity, load-moment capacity and developed FE models have been checked with respect to experimental results.

1.4 Organization of Thesis

This thesis has been organized in six chapters. **Chapter 1** includes the background of the work along with the objectives and scope of the current study. An extensive literature review has been done to figure out the key parameters that have an immense influence on the behavior of steel angle and strip jacketed RC columns. A comparative study has also been done from the published experimental works to compare the effects of different governing parameters. Published analytical models have also been studied in this segment. These review part has been reported in **chapter 2**.

Chapter 3 contains the details of description of experimental specimens, material properties, fabrication of specimens and test module. **Chapter 4** includes the details of finite element modeling process.

Chapter 5 represents all the output of this study which includes effect of eccentricities experimentally and numerically as well as performance of analytical models. Finally, the summary and conclusions of the work along with the recommendations for future research have been included in **chapter 6**.

2.1 Introduction

Infrastructure rehabilitation or strengthening of existing structure is one of the most important works for civil engineers. It may include individual element (i.e. column, beam etc.) strengthening to overall strengthening of structure. Individual structural element strengthening may be done using Reinforced Concrete (RC) jacket, Fiber Reinforced Polymer (FRP) or Steel jacket etc. Strengthening in a cost effective way is very important for developing countries like Bangladesh since modern rehabilitation materials e.g. FRP are very expensive. FRP materials are also not efficient as the eccentricity rises (Țăranu *et al.*, 2011). Steel angle and strip (also known as steel cage) strengthening method is relatively cost effective because of its low cost and availability. This type of steel jacketing consists of four angles attached with corners of column and discrete horizontal steel plates with a specific spacing which are welded to the angles. Figure 2.1 shows the salient features of a steel cage jacketed RC column. Throughout this article steel jacketing and strengthening will be used synonymously.

Several researchers studied steel jacketing with steel angles and strips due to its effectiveness to increase load carrying capacity and simplicity in installation. They carried out experimental programs to study the effect of key parameters including length of angle, bonding agent between angle and concrete, strip spacing, length of angle etc. of steel jacketed RC column. Based on experimental results, some analytical models have been introduced for the prediction of load capacity. Several researchers also gave effort to investigate the performance of finite element modeling to predict the behavior of RC column jacketed with steel angles and strips. From literature the deficiency found in the area of research about the behavior of steel angle and strip jacketed RC column under eccentric loads.

In the following section, a brief review of available studies and comparative study of influences of different key parameters on the capacity of steel angle and strip jacketed RC column have been reported.

2.2 Theoretical Strength Restoring Mechanism

2.2.1 Concrete confinement

The capacity of concrete can be increased by giving a confinement to the member which delays the onset of crushing. Concrete confinement can be classified as active and passive. In active confinement, the confining pressure is applied to prestress the concrete element prior to loading (Shin and Andrawes, 2010). It can be achieved by using steel bands or FRP wraps, where jacketing materials should be prestressed in some manners.

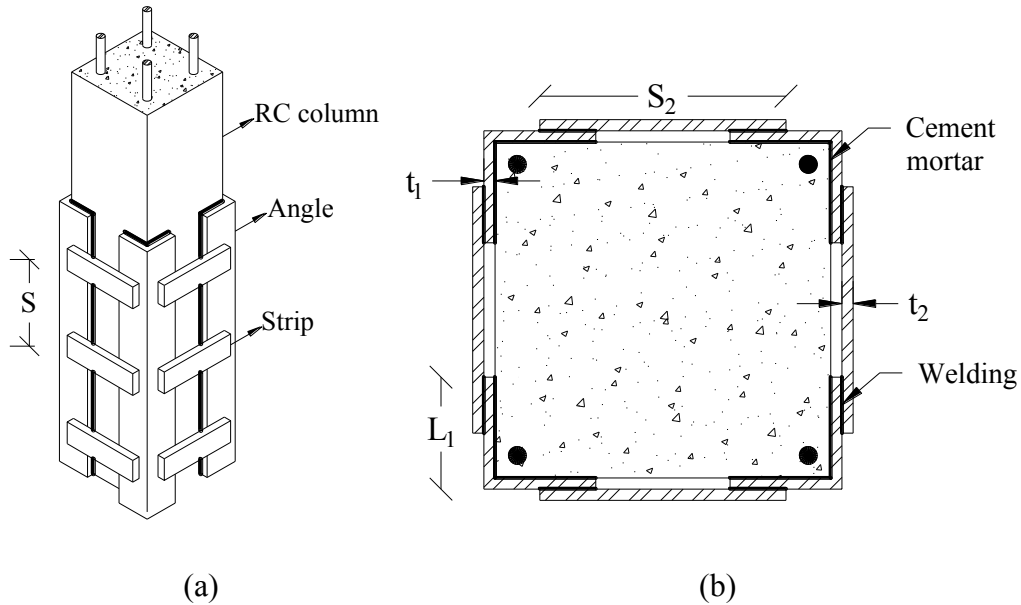


Figure 2.1 Schematic diagram of steel angle and strip strengthened RC column
(a) Elevation and (b) Cross section

On the other hand, in passive confinement the confining pressure is activated as a result of concrete dilation due to applied loads (Shin and Andrawes, 2010). Passive confinement can be applied on concrete elements using steel jackets or FRP. In steel angle and strip strengthened RC columns, concrete passive confinement is generated because of the

constraint provided by steel cage to expand concrete laterally. Concrete expansion is induced by the Poisson's effect under axial loads. When compressive stress of concrete in the strengthened column approaches to the uniaxial compressive strength, lateral strains become very high due to progressive cracking (Nagaprasad *et al.*, 2009). Afterward, strips come into action to take the tensile forces which delays the failure. Generally confinement effect in terms of confining pressure is highest near the area of strips. This fact is illustrated in Figure 2.2 (a), which shows that close to strips effective confining band is larger and area in between strips are less effective in confinement. Confining pressure also varies along the length of strips (Figure 2.2 (b) and 2.2 (c)). Distribution of confining pressure on the plane of strip level as well as along the length of angles is the point of interest of many researchers (Nagaprasad *et al.*, 2009; Badalamenti *et al.*, 2010; Calderón *et al.*, 2009; Braga *et al.*, 2006) who provided analytical models for the confinement.

2.2.2 Composite action

Steel angles' contribution can be incorporated to predict the strength of jacketed columns considering the composite action. In this concept, angles are assumed to be under axial load and bending moment (Figure 2.3). The axial load comes from the shortening of column in case of directly loaded column or from friction occurring at strip levels in case of indirect loading. Bending moment is induced by the expansion of concrete (Badalamenti *et al.*, 2010). Several researchers (Calderón *et al.*, 2009; Braga *et al.*, 2006) attempted to quantify the contribution in different manners which will be discussed later.

2.3 Experimental Investigation

Tarabia and Albakry, 2014 conducted an experimental program consisting of 10 samples to study the behavior and effectiveness of RC columns strengthened by steel angle and strip. Parameters considered in the study were the size of the steel angles, strip spacing, grout material between column sides and angles, and the connection between the steel angle and specimen head. The failure in the specimens started with the buckling of the one or more of the vertical angles followed by the buckling of the reinforcement steel bars and eventually a crushing of concrete section near these bars (Figure 2.4). Several points have been

concluded from the study. The enhancement of ultimate load capacity comes from the resistance capacity of corner angles and confinement provided by strips. The ductility of jacketed column increases in most of the cases at least 50% which indicates the effectiveness of this strengthening procedure in seismically deficient columns. To be economical, the usage of cement as binder between steel angle and old column surface has been recommended.

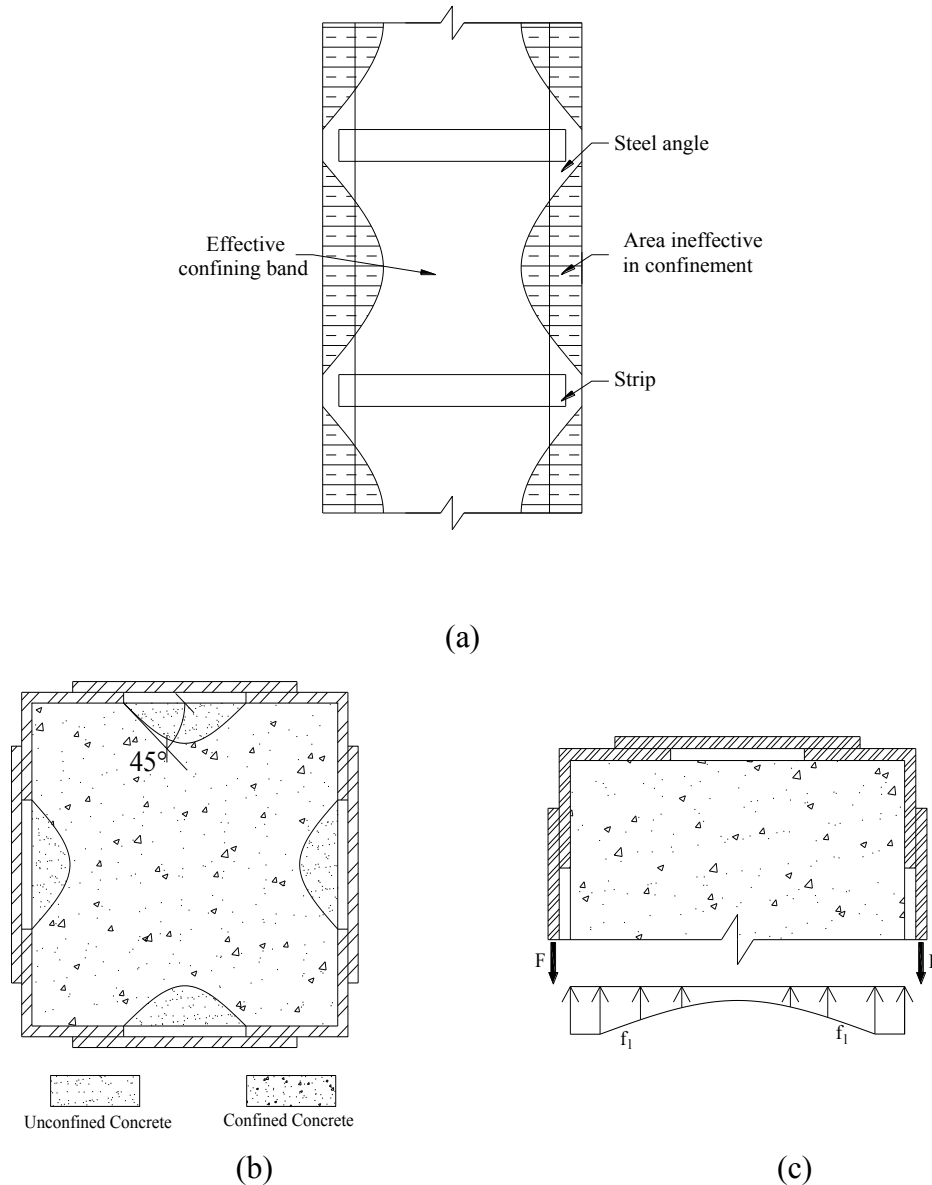


Figure 2.2 Confinement due to steel cage (a) effective confinement in elevation, (b) confinement pressure distribution at strip level, and (c) effective confinement in plan (Redrawn from Nagaprasad *et al.*, 2009)

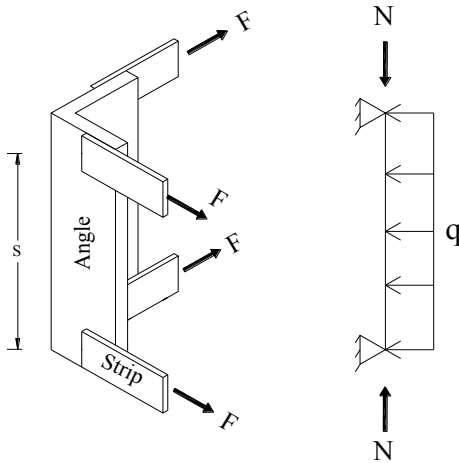


Figure 2.3 Schematic diagrams of loads on steel angle (Redrawn from Badalamenti *et al.*, 2010)



Figure 2.4 Failure modes of jacketed columns with buckling of corner angle

Abdel-Hay and Fawzy (2015) studied the effect of partial strengthening of defected RC columns using different strengthening procedures, where two samples were jacketed using steel angle and strip. Result followed the study demonstrated that an increase in the height of jacket (i.e. length of angle) subsequently improves both the ultimate load capacity and ductility. Failure occurs outside of the strengthened zone (Figure 2.5).



Figure 2.5 Failure at un-strengthened part of partially jacketed columns

Khalifa and Al-Tersawy (2014) designed an experimental program with seven column samples to evaluate the enhancement in load capacity, stiffness and ductility. Performance of steel angles and battens strengthening method has been evaluated by comparing it with other steel caging jacketing method (i.e. using four steel plates on the faces of column). The conclusive remarks depict that the increase of load capacity and ductility mainly depend on strip thickness, whereas the stiffness depends on strip thickness and spacing. The failure may occur when the steel cage yields and concrete between the strips is splitting out (Figure 2.6). An analytical model has also been formulated in the study which will be discussed later.



Figure 2.6 Failure of jacketed column by concrete splitting

Elasamny *et al.* (2013) carried out experiments on the steel angle and strip jacketed columns which were loaded eccentrically. Focus has been given mainly on the parameters of eccentricity, angle area and number of strips. Result followed the study indicate a decrease in load carrying capacity of the strengthened column due to the increase in eccentricity. The decreases were within the ranges of 10-40%, depending on the number of strips. The study gives an important aspect for future research as it has been found that the non-effectiveness of number of strips. Though it seems to be irrational (also acknowledged by the authors) but non-effectiveness has been remarked as a consequence of large spacing of strips used in the study. Therefore, recommendation has been proposed for the future study about the maximum spacing of strips. The modes and location of failure of jacketed RC columns has also been investigated (Figure 2.7).

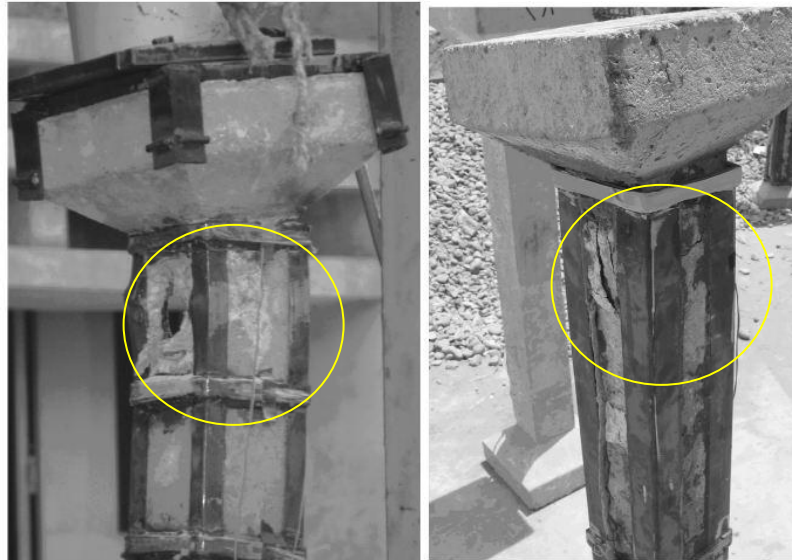


Figure 2.7 Failure of jacketed column under eccentric loading

Campione (2011) mainly focused on the analytical model formulation but conducted an experimental work to verify the derived analytical model and to observe the effect of the batten spacing. It has been concluded that the directly loaded strengthened column acts as a composite member, in which both confinement effect and composite actions are present. The obtained results showed that the ductility of strengthened columns increase with the decrease of batten spacing.

Areemit *et al.* (2013) has studied distinctively the effect of batten configuration of steel angle and batten strengthened columns. Batten spacing has been changed without altering area of steel throughout the height of column. It has been found that the confinement at ends has a significant role to increase load carrying capacity and the increase in the shear transfer length between steel angle and concrete core subsequently results the dominance of composite action.

Giménez *et al.* (2009) conducted an experimental work to investigate the influence of the strips configuration on the steel angle and strip jacketed RC columns. Number of strips was increased in the possible failure zones (predicted from author's previous work), which leads to an increase in the ultimate load capacity. The load condition i.e. loaded or unloaded during strengthening was also a parameter of this study. Results showed that unloading during strengthening is preferable to increase the load capacity of strengthened column.

Giménez *et al.* (2009) carried out test consisting of 14 strengthened columns using steel angle and strip. The objective of the study was to investigate the effect of the loading and unloading state of column during strengthening; effect of using epoxy or cement mortar as binder between concrete and steel angle and the effect of capital on load transmission to the column. Conclusion followed the results declines the composite behavior of the steel angle and concrete at the ends of column. It has also been concluded that epoxy mortar has negligible effect on the load capacity and unloading is preferable before strengthening to improve capacity.

Delgado *et al.* (2005) studied RC columns retrofitted by different methods experimentally under cyclic loads. Steel angle and strip jacketed RC columns showed slightly improved behavior than steel plate jacketed columns. This happens due to the use of angles profiles connected by strips at the corners which delays the cover concrete spalling specially in the critical zone.

Dolce *et al.* (2003) studied different local strengthening method on 24 column specimens to investigate the role of confinement on ductility and strength. They also carried out Cyclic loading-unloading compression tests on strengthened and not strengthened columns has also

been carried out. The conclusive remarks indicate the ductile behavior and strength at large displacement of steel angle jacketed column than FRP jacketed column.

2.4 Numerical Investigation

Adam *et al.* (2009) investigated the performance of Finite Element models of steel angle and strip jacketed RC columns. 1/8 th portion of specimen jacketed concrete column has been modeled in ANSYS using the benefit of symmetry to simulate experimental works. Solid, link, and shell elements have been used to model concrete, reinforcement, and steel cage respectively. Reinforcements have been assumed to be smeared in concrete. Contact between angle and concrete has also been considered in the models. A maximum difference of 5% was observed between experimental and numerical result which indicates a good agreement.

Garzon-Roca *et al.* (2012) studied numerical simulation using quarter model of jacketed column in FEM software ABAQUS. Concrete and steel plates have been modelled with solid elements. Two nodes truss elements have been used to model reinforcements and considered embedded in concrete mass. Hard contact with tangential friction has been considered in between concrete and steel cage. FE modeling of jacketed column indicates a good match with experimental results with a standard deviation of 0.082.

Belal *et al.* (2015) carried out numerical analysis of half scale jacketed column model using FEM software ANSYS. To model concrete and steel plate solid elements have been used. Models predicted failure, failure loads and displacements very close to experimental results. The study concluded that finite element models overestimated failure loads compared to experimental results.

2.5 Analytical Models

Khalifa and Tersawy (2014) proposed an analytical model (Equation 2.1) to predict the load capacity of steel angle and strip strengthened RC column taking into account the composite action of core concrete and local buckling of steel elements. The confinement provided by steel angle and strip assembly has been taken into account. The relation between confined and unconfined concrete compressive stress was adopted from Li, Gong and Wang (2009). Concrete confinement has been incorporated by the factor m_c , shown in Equation 2.2. To incorporate the contribution of steel angles in capacity, a continuous supported (at strips) beam with axial and bending loads has been considered. These loads may result in buckling of steel angle and/ or axial deformation of strips. A reduction factor, m_s (Equation 2.3) to yield stress has been prescribed to consider this effect.

$$P_{ult} = m_c \cdot f_c \cdot b^2 + m_s \cdot A_s \cdot f_{yl} \quad (2.1)$$

$$m_c = \frac{f_{cc}}{f_c} = 1 + 2.15 \left(\frac{2 \cdot t_s \cdot s_2 \cdot f_{yl}}{S \cdot b} \right) \quad (2.2)$$

$$m_s = \frac{8.47}{2 \cdot L_1 \cdot t_1} \sqrt{E_r \cdot t_1 (\alpha L_1)^3 \frac{s_2 \cdot t_2 \cdot E_h}{b \cdot S}} \quad (2.3)$$

Tarabia and Albakry (2014) prescribed a very simple analytical model to assess the load carrying capacity of strengthened RC columns. This model assumes rigid corner angles which may not buckle before the onset of yielding and have any flexural deformation. The confined concrete stress model (Equation 2.4) by Badalamenti *et al.* (2010) has been adopted. Confinement pressure shown in Equation 2.5 has been derived considering deformation compatibility of concrete column and steel cage using the similar approach of Calderón *et al.* (2009).

$$f_{cc} = \left[f_{co} \left(1 + 3.7 \left(\frac{f_l}{f_{co}} \right)^{0.87} \right) \right] \quad (2.4)$$

$$f_l = \frac{N_c}{b^2} \frac{\nu_c}{\left(1 - \nu_c + \frac{b.S.E_c}{2.l_2.t_2.E_s}\right)} \quad (2.5)$$

Contribution of steel angles to ultimate capacity has been calculated for direct and indirect loading of strengthened column considering the shortening of column and friction respectively. Expression of angle capacity for one corner angle can be found using Equation 2.6 and Equation 2.7 for direct and indirect loading respectively.

$$N_a = 2.L_1.t_1.f_y \quad (2.6)$$

$$N_a = \sqrt{2}.f_l.b.S.\mu, \text{ Where } \mu = 0.5 \quad (2.7)$$

Campione (2011) proposed a model for the design of concrete column strengthened by steel angles and battens considering direct and indirect loads on angles. This model considers the contribution of confinement pressure and load capacity of steel angle, in case of direct loading, to determine the compressive strength. To determine the confining pressure, it has been assumed that the confinement pressure decreases suddenly in steel battens (Figure 2.8), whereas it remains almost uniform along the length of angle, which is a finding of author's previous work. Finally, a simplified confinement pressure measurement has been prescribed which is justified for the case of lower stiffness of battens than the corner steel angles.

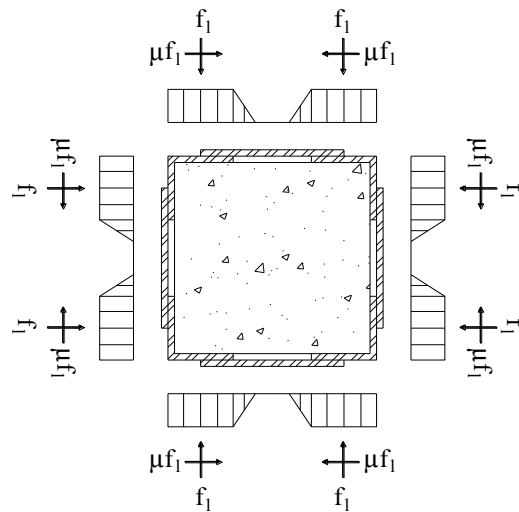


Figure 2.8 Confining pressure distributions at batten level (Redrawn from Campione, 2011)

The contribution of steel angles to the load capacity has been measured considering the coupled effect of axial and bending forces on the angles. The axial force comes from the shortening of column and flexural force comes from the reduction of lateral expansion of column due to confinement. Considering confinement pressure and composite action, axial capacity (P_{ult}) of directly loaded RC column strengthened with steel angle and batten is as Equation 2.8.

$$P_{ult} = n \cdot f_{cd} \cdot A_c + n_a \cdot 8 \cdot L_1 \cdot t_1 + A_{st} f_{yl} \quad (2.8)$$

where, n is dimensionless load carrying capacity of confined concrete core (Equation 2.9) and n_a is the maximum axial force available in directly loaded angles in the dimension less form (Equation 2.10).

$$n = \frac{f_{cc}}{f_{cd}} = 1 + 1.42 \left\{ \frac{4 \cdot t_2 \cdot S_2}{b \cdot S} \frac{f_{ydb}}{f_{cd}} e^{[-1.5 \frac{s}{b}]} \right\}^{0.87} \quad (2.9)$$

$$n_a = \sqrt{\left[1 - 0.63 \frac{1}{t_1} \frac{S}{b} \frac{1}{\frac{L_1}{S \cdot t_1} + \frac{(0.5b - L_1)}{s_2 t_2}} e^{[-1.5 \frac{s}{b}]} \right]} \quad (2.10)$$

Campione (2013) proposed simple analytical model for the hand calculation of capacity of strengthened RC column at pure compression, pure axial force and balance condition. Strain compatibility of section and undistorted plain section has been assumed in this model. Finally, the analytical model has been verified with test data available in the literature which gives good agreement.

Calderón *et al.* (2009) formulated analytical model for the design strength of axially loaded RC columns strengthened with steel angle and strip. This model considers confinement provided by the angle-strip combination and failure mechanism of strengthened column i.e. yielding of angles or strips. The ultimate load of the strengthened column can be expressed as Equation 2.11.

$$P_u = 0.85 A_c \cdot f_c + A_s \cdot f_{ys} + K_f \cdot A_c + N_L \quad (2.11)$$

In this mathematical model, the parameter K reflects the effect of higher compressive strength of concrete due to confinement pressure (f_i) and N_L represents the loads taken by the steel angles. The axial load transmitted to the cage at the end of strips can be expressed by Equation 2.12.

$$N_L = N_o(1 - e^{-ms^2}) \text{ Where, } m = \frac{4 \cdot \mu \cdot v_c}{b \cdot (1 - v_c + \frac{b \cdot E_c}{2t_2 E_L})} \quad (2.12)$$

The confinement can be expressed by the Equation 2.13 and Equation 2.14 depending on the failure.

$$\text{In case of yielding of angles } f_i = \frac{16 \cdot M_p \cdot \sqrt{2}}{(S - S_2)^2 \cdot b} \quad (2.13)$$

$$\text{In case of yielding of strips, } f_i = \frac{2 \cdot t_2 \cdot S_2 \cdot f_y}{b \cdot S} \quad (2.14)$$

The ultimate load calculation is an iterative process because each angle and strip has the chance of failure at pick point. So it is necessary to check the possibility of yielding of all the angle sections located between two strips as well as each of the strips involved. Ultimate capacity will be the lowest possible ultimate load calculated for different failure mechanism. The values of μ and K were adopted from the Adam *et al.* (2009) as 0.20 and 2.5 respectively.

Eurocode 8 (2003) gives design formula for the load carrying capacity of steel angle and batten strengthened RC column. The proposed design strength (Equation 2.15) takes the contribution of confinement at batten level and discontinuities of batten in the load carrying capacity. The contribution of the corner steel angles to resist loads has been ignored.

$$P_{ult} = f_{cd} \cdot b^2 \cdot \left(1 + 2.02 \left\{ w_s \left[1 - \frac{2}{3} \frac{(b - 2L_1)^2}{b^2} \right] \cdot \left(1 - \frac{s}{2b} \right)^2 \right\}^{0.87} \right) \quad (2.15)$$

where, $w_s = \rho_s \frac{f_{ydb}}{f_{cd}}$

Campione (2013) proposed analytical model for a three point interaction diagram of steel angle and strip jacketed RC column. These three points are of capacity under pure compression, flexure, and at balance failure. Analytical derivation was made assuming equivalent stress-block parameters for internal force considering the confinement effect induced in concrete core by external cages. Simple analytical equations have been proposed on the basis of constitutive laws of confined concrete and steel angles. The proposed model has been verified by available experimental data with good agreement. So, the study concluded that the proposed model allows hand control of the influence of main parameters governing the behaviour (angle and strip geometry and mechanical properties of constituent material) of RC columns externally strengthened with steel cages.

2.6 Comparative study of the Influence of Key Parameters

From the experimental works and analytical models it is obvious that strip spacing along with thickness and configuration, cross section of steel angles, connection of steel angles to specimen head, grout material, eccentricity have the control over the ultimate load capacity of steel angle and strip jacketed RC columns. In this section comparative study has been conducted to observe the effect of governing features on the strengthened column at a glance. Data available in the literature (Appendix Table A.1 and A.2) are used to conduct the study of the following sections.

2.6.1 Grout material

Cement or epoxy can be used to fill the gap between steel cage and existing column surface which ensures a continuous contact. Stress induced by the column shortening in steel angle depends on the bonding agent provided. Tarabia and Albakry (2014) conducted a study in this regard which shows that the change in compressive behavior is not enormous (Figure 2.9). So the use of cement as grout material rather than epoxy has been recommended. Similar conclusion has been drawn by Giménez *et al.* (2009).

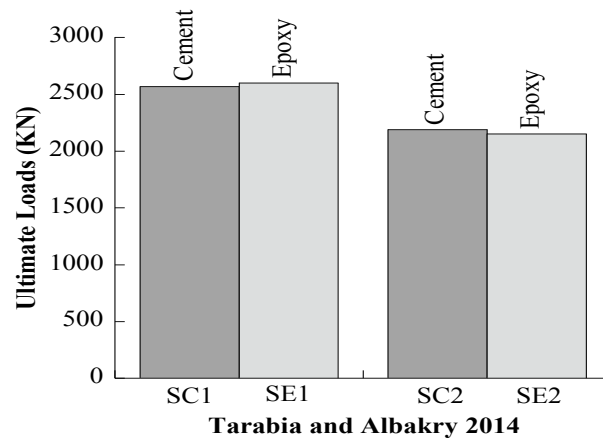


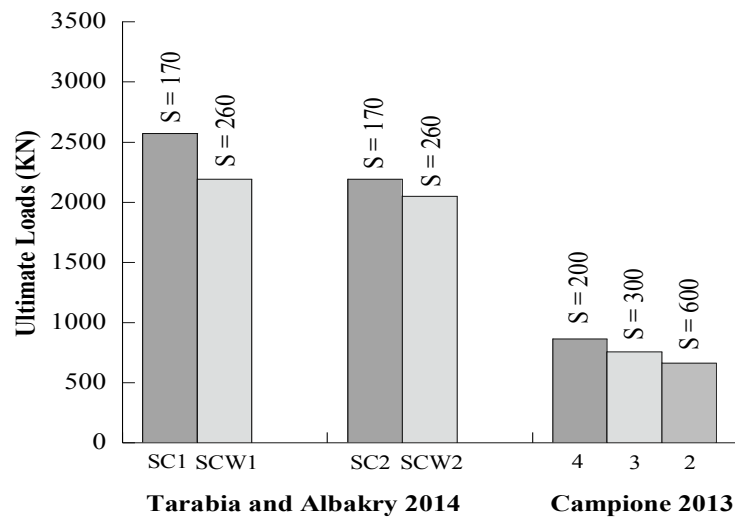
Figure 2.9 Effect of grout materials on the ultimate load capacity

2.6.2 Strip configuration

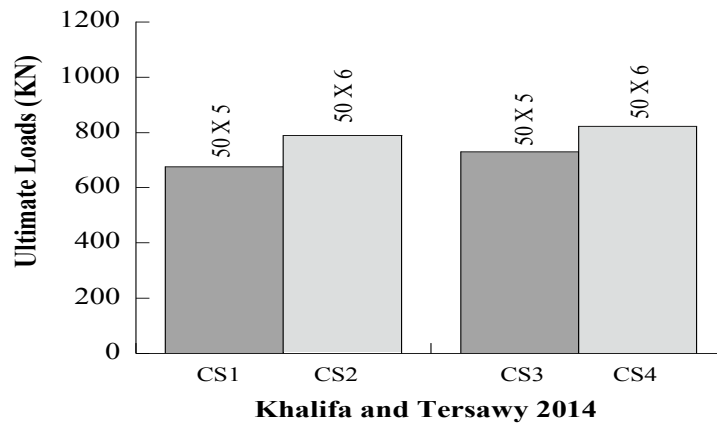
Strips are provided to get confinement and to resist buckling of steel angles. Strip configuration including spacing and thickness of strips is the single most important parameter that has profound effect on the failure location of strengthened RC column. Strips are generally spaced equally along the length of column. But Giménez *et al.* (2009) shows that additional two strips of smaller section at top and bottom increase the load capacity significantly than the equally distributed strips. Also, Elsamny *et al.* (2013) conducted investigation to observe the effect of strip distribution. Specimens with unequally distributed strips were tested, in which strips are closely spaced at the top and bottom whereas one strip at the middle of specimen. The failure occurred in between widely spaced strips. Strip thickness also affect the confinement therefore load capacity. Figure 2.10 (a) and 2.10 (b) display the effect of strip spacing and strip thickness on the ultimate capacity. The ultimate capacities of jacketed RC columns change within a range of 6 to 11 and 12 to 16 percent for strip spacing and strip thickness respectively. Ductility of strengthened RC column also increases with the decrease of strip spacing (Campione, 2011).

2.6.3 Angle size

Steel angle and strips are generally provided to get passive confining pressure. But steel angles have to take axial loads which come through the frictional shear transfer and due to shortening of column. Figure 2.11 shows the effect of change in steel angles' cross section on the load capacity and the changes are within 4 to 8 percent. It also affects the crushing and loss of cover at failure. Wider steel angles result in less crushing and loss of cover due to more confinement though failure mode remain the same as with the narrow angle (Elsamny *et al.*, 2013).



(a)



(b)

Figure 2.10 Effect of (a) strip spacing and (b) strip thickness on the ultimate capacity

2.6.4 Connection to specimen head

Connection of steel angles to the specimen head can be used to simulate the real connectivity. Direct loading approach is appropriate to simulate the situation where it is feasible to connect steel angles to slab and beam. Indirect loading is appropriate where connection between angles and slab is not feasible. In case of direct loading angles reach yield before failure so ultimate load capacity increases within a range of 9 to 29 percent, as shown in Figure 2.12.

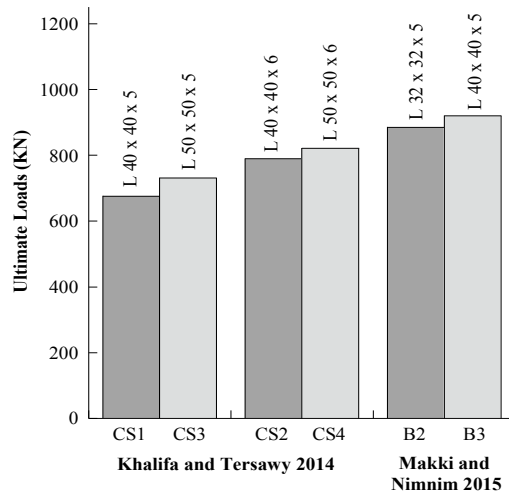


Figure 2.11 Effect of angle size on ultimate load capacity

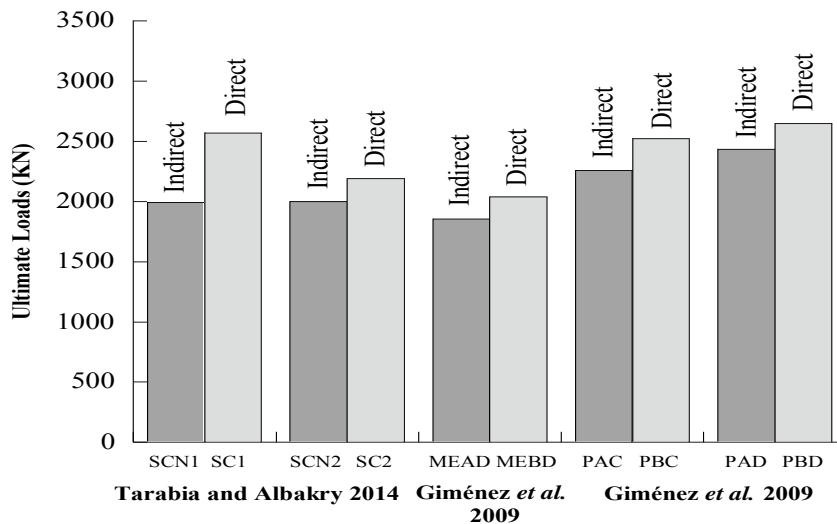


Figure 2.12 Effect of angles and specimen head's connectivity on ultimate load capacity

2.6.5 Eccentricity

Elsamny *et al.* (2013) investigated the behavior of strengthened column under eccentric loads especially. The results found indicate that ultimate load capacity decreases (Figure 2.13) with the increase of the eccentricity. The decreases are within a range of 34 to 41 percent as the eccentricity changes from 8.33 to 33.3 percent. This behavior can be attributed to higher axial strain of angles at the side of eccentric load due to higher eccentricity. Subsequently angles yield faster at higher eccentricity with less ultimate capacity. This has been also found in the study that the contribution of angles (P_{angle}) to the ultimate capacity (P_{ult}) decreases with the increase of the eccentricity (Table 2.1).

Table 2.1: Contribution of steel angles to ultimate load capacities

Reference	Model	Eccentricity, e/b (%)	P_{ult} (KN)	P_{angle} (KN)	$P_{\text{angle}}/P_{\text{ult}} \times 100$ (%)
	C1T3	8.3	390	31	7.95
Elsamny <i>et al.</i> (2013)	C4T3	16.6	290	22	7.59
	C7T3	25.0	255	16	6.27
	C10T3	33.3	175	6	3.43

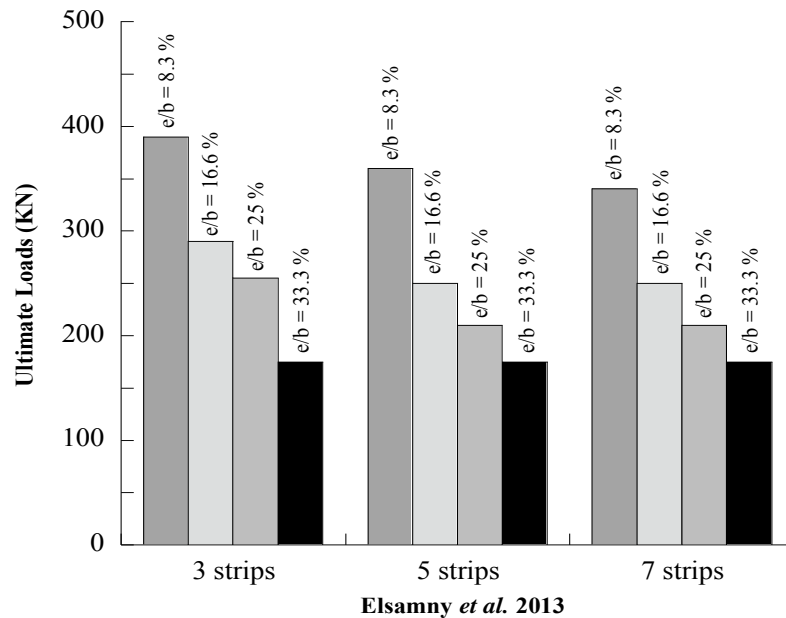


Figure 2.13 Effect of eccentricity of loading on the ultimate load capacity

2.6.6 Length of retrofiting

RC column jacketing is a local strengthening method which develops passive confinement pressure and provides composite action. To get proper confinement retrofitting length should be adequate. Abdel-Hay and Fawzy (2015) studied the effect of partial strengthening using different strengthening methods. Among samples two sample encoded as CS5 and CS6 (Table 2.2) were jacketed with steel angle and strips with partial and full height strengthening respectively. It has been reported that increase in the retrofitting zone has advantages on the capacity and ductility of strengthened column. Areemit *et al.* (2013) found that stress in the steel angles is higher at the mid height and reduces at the ends, which indicates the partial development of composite action. It has been concluded that composite action may not develop fully due to insufficient development length of concrete and steel angles in case of partial strengthening. So, recommendations have been prescribed for the use of long steel angle to get the composite action with better shear transfer capability.

Table 2.2: Effect of length of angles on the ultimate load capacity

Reference	Model	Corner Angles (L ₁ xL ₁ x _t ₁) (mm)	Steel Jacket Length (mm)	Ultimate Load (KN)	Increase in Ultimate load (%)
Abdel-Hay and Fawzy (2015)	CS5	40 x 40 x 4	500	591	83
	CS6	40 x 40 x 4	750	843	131

2.6.7 Load State during strengthening

Initial stresses on the RC column, which is to be retrofitted, have some influences on the behavior of repaired column. Sometimes, sample columns have to be preloaded before test to simulate real structure. Ductility of preloaded columns is less than non-preloaded columns (Ong and Kang, 2004). Unloading of structure before strengthening of columns is not feasible always. To demonstrate the effect of unloading along with other parameters Giménez *et al.* (2009) designed an experimental program. It has been concluded, based on the obtained results (Figure 2.14), that effect of unloading before strengthening is

insignificant in case of 70% preloading. The changes in ultimate capacity have been within 4 to 7 percent. The effect may increase for the higher preloading.

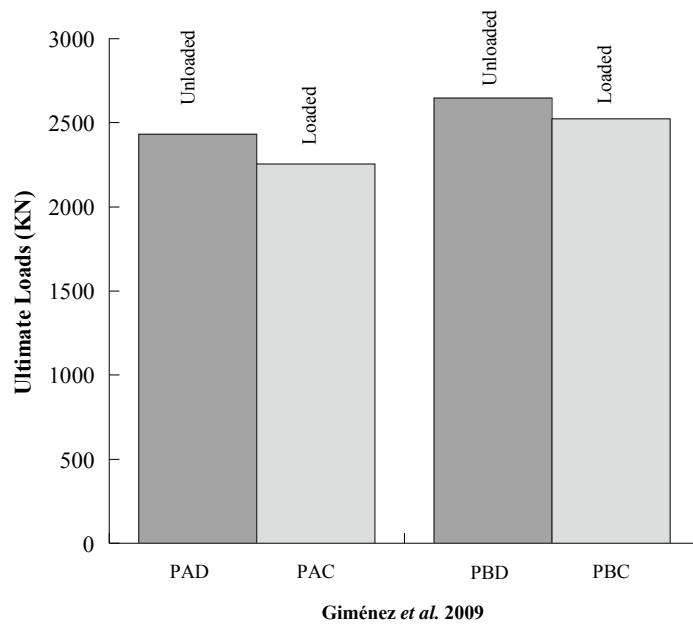


Figure 2.14 Effect of load state during strengthening on the ultimate load capacity

2.7 Conclusions

Column strengthening is a quick solution to mitigate the deficiency of load carrying capacity of RC columns. Strengthening by steel angle and strip is the easiest and also an effective method among all other methods. From this study following conclusions can be drawn-

1. Studies on the behavior of steel angle and strip jacketed RC columns under eccentric load are insufficient.
2. Several analytical models are established to predict the compressive capacity of steel angle and strip strengthened RC square columns. But the deficiency found in the capacity prediction model for eccentrically loaded strengthened RC columns as well as the formulation formula for interaction diagram.

3. The comparative study indicates that strip configuration, loading approach on steel angle and length of retrofitting zone are the key parameters that have profound influences on the capacity of steel angle and strip strengthened RC column.
4. The effects of preheating of strips before welding are stated in researches but not studied at all in a large extent.

3.1 General

This study has been conducted to investigate the behavior of steel angle and strip jacketed RC columns under eccentric axial loads. More specifically, study has been intended to investigate the effect of load eccentricity on the load carrying capacity, ductility, confinement stress, mid-height displacement etc. of the steel angle and strip jacketed RC columns. To achieve these objectives, an experimental program has been designed. In the program, six RC columns have been constructed with same long and transverse reinforcement configuration. After that, five RC columns have been strengthened with similar external steel cages. The steel cage consists of four vertical steel angles installed at the corners of the column joined by horizontal steel strips at a certain interval. Finally, un-strengthened and strengthened RC columns have been tested in the laboratory to identify their behavior under eccentric loads. In addition to that, further effort has been given to model samples in Finite Element platform to acquire complete behavior, which will be discussed in the next chapter.

3.2 Description of Test Specimens

Six half scale RC columns measuring 150x150x1500mm have been constructed. Among them, five columns have been jacketed with 50x50x5mm angle at corners and 125x50x5 mm strips at certain interval. The cross section of strengthening steel has not been scaled down, which is a limitation of this study. One column has been kept as a control column without jacketing. Table 3.1 shows the details of the specimen configuration. Angles have been bonded with the sides of RC column with cement mortar. Strip spacing at the middle 900mm has been kept 150mm, whereas top and bottom 300mm portions have lower spacing. It has been introduced to avoid failure at top and bottom. Strips have been welded with the angles properly to avoid local shear failure. 10mm diameter longitudinal

reinforcement along with 8mm diameter ties at an interval of 150mm has been embedded in RC core. Details of the column jacketing technique using steel angle and strip have been illustrated in Figure 3.1.

Table 3.1: Details of the test specimens

Specimen	Angle size (mm)	Strip size (mm)	Strip spacing at middle (mm)	Reinforcement		Load Eccentricity, e (mm)
				Longitudinal (mm)	Tie (mm)	
CA1	-	-	-	4- ϕ 10	ϕ 8	0
CA2	50x50x5	125x50x5	150	4- ϕ 10	ϕ 8	0
CA3	50x50x5	125x50x5	150	4- ϕ 10	ϕ 8	15
CA4	50x50x5	125x50x5	150	4- ϕ 10	ϕ 8	37.5
CA5	50x50x5	125x50x5	150	4- ϕ 10	ϕ 8	67.5
CA6	50x50x5	125x50x5	150	4- ϕ 10	ϕ 8	Bending

3.3 Explanation of Test Parameter

Test specimens CA1 through CA6 were designed with similar geometric and material properties. The control column specimen CA1 has been keptunjacketed and tested under concentric loads. Test columns CA2 through CA6 have been jacketed with the same configuration of steel angles and strips. They have been tested under different load eccentricities varying from zero to infinity, which has been imposed during the load application. After testing, data acquisition has been done to investigate mainly the ultimate load capacity, displacement ductility and failure modes etc.

3.4 Material Properties

3.4.1 Cement

Standard Portland Composite cement branded as Scan cement has been used to construct all test columns.

3.4.2 Aggregate

Locally available brick chips of one inch downgrade and sand have been used as coarse aggregate and fine aggregate respectively. Properties of aggregates, necessary for the mix design have been determined from the laboratory tests and are presented in the Table 3.2. The gradation curve of the fine aggregate is given in Figure 3.2.

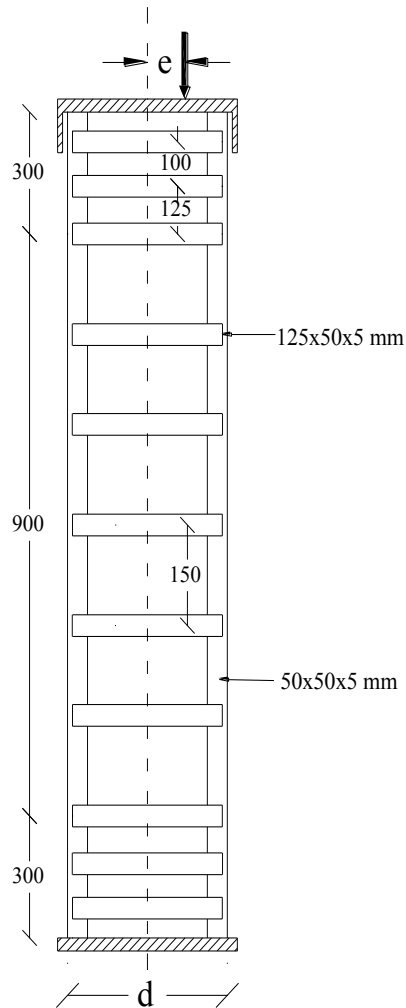
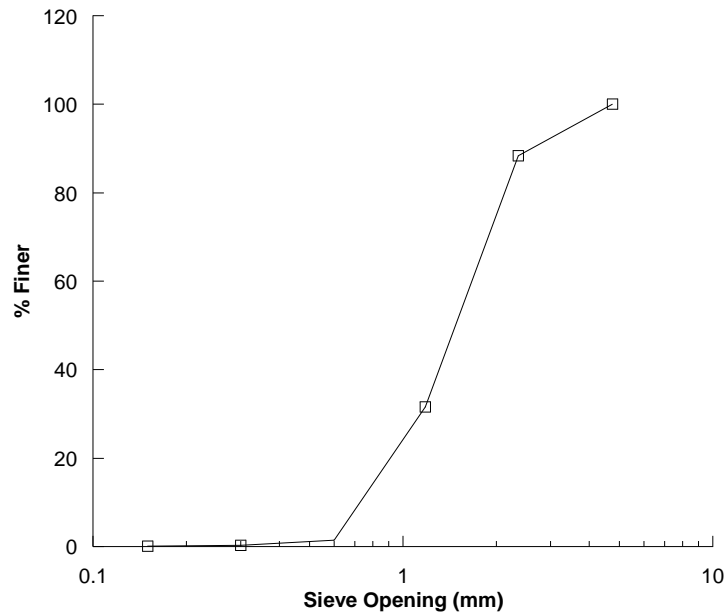


Figure 3.1 Typical steel angle and strip jacketed RC column

Table 3.2: Properties of aggregates

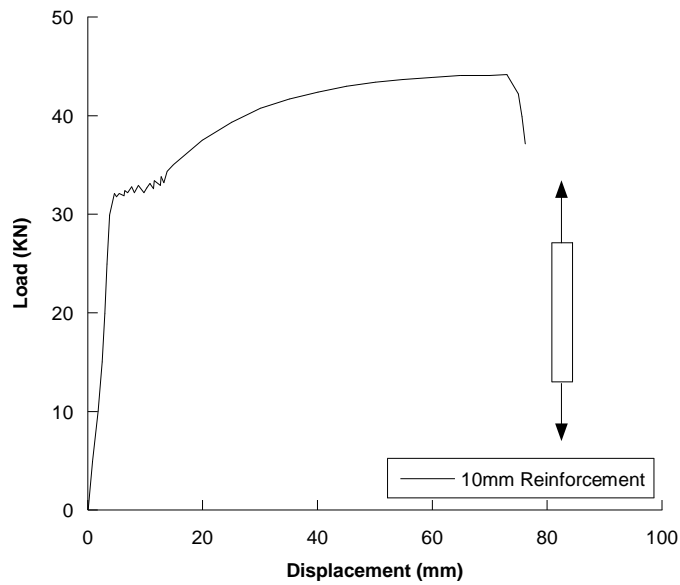
Properties	Coarse aggregate	Fine Aggregate
Dry rodded unit weight (Kg/m ³)	1104	-
Bulk Specific gravity (SSD)	1.95	2.40
Absorption capacity (%)	16.16	4.27

**Figure 3.2** Gradation curve of fine aggregates**Table 3.3: Properties of steel elements of jacketed RC columns**

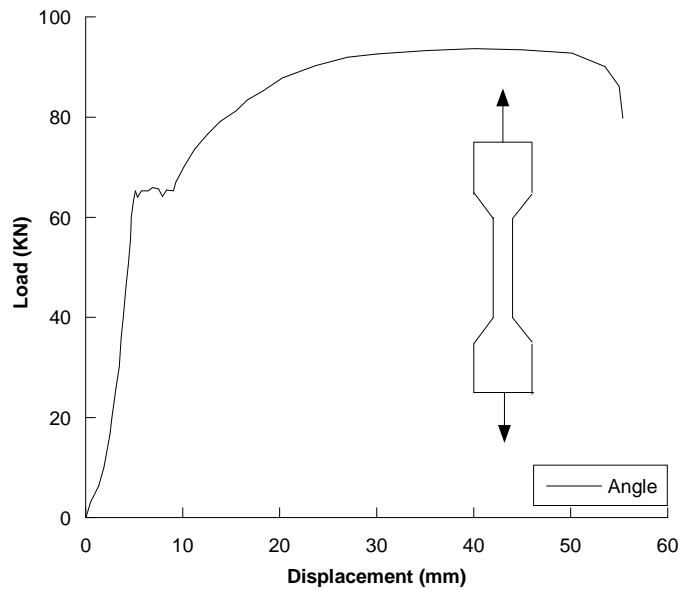
Properties	Reinforcement		Angle	Strip
	10mm v	8mm v		
Yield stress (MPa)	409	576	449	380
Yield strain (mm/mm)	0.00204	0.00288	0.00224	0.00190
Ultimate stress (MPa)	556	647	624	493
Ultimate strain (mm/mm)	0.19	0.02	0.19	0.18

3.4.3 Reinforcement

10mm and 8mm diameter deformed bars branded as ASRM 300 have been used as long and tie reinforcements respectively. Properties of the steel reinforcements have been shown in the Table 3.3. Load deflection curve of the 10mm diameter bar has been shown in Figure 3.3 (a).



(a)



(b)

Figure 3.3 Load-deflection curve of (a) 10mm diameter reinforcement and (b) Steel angle

3.4.4 Steel angle and Strip

50x50x5mm angles branded as “VSL Xsuper 345” has been used in this study. 50x5mm strips having a length of 125mm have been used to tie the angles. Properties of angle and strip have been provided in the Table 3.3. The load deflection curve of the coupon test of angle section is shown in Figure 3.3 (b).

3.5 Test Column Fabrication

3.5.1 Concrete mix design

The main focus during mix design was to make a relatively low strength concrete. Locally available materials have been used to make the concrete mix. Properties of all materials are given in the previous section. Mix design was done assuming 25-50 mm slump value and 1 inch downgrade course aggregate using ACI method. Water to cement ratio was kept 0.60 to get a lower strength concrete. The materials required as per mix design is presented in the Table 3.4.

Table 3.4 ACI Concrete mix design at Saturated Surface Dry (SSD) Condition

Materials	Weight (Kg)	
	For one cum of Concrete	For one Batch
Cement	240	28
Sand	834	96
Brick chips	723	83
Water	144	17

3.5.2 Concrete placement and curing

As per specified mix design ingredient materials have been mixed with mechanical concrete mixture. Specimens were cast in three batches where two columns and two cylinders were cast in each batch. Cylinders have also been cast for the compressive strength test. After mixing concrete slump test has been performed to check the workability and verify the assumed value. After that, concrete has been cast in the prepared horizontal formworks.

Casting has been performed in two layers with compaction by the vibrator. Glimpse of major steps has been shown in Figure 3.4 (a) through Figure 3.4 (f). RC columns have been cured with water after the day of casting for 28 days. To avoid surface water evaporation jute and polyethene sheets have been used.



(a)



(b)



(c)



(d)



(e)



(f)

Figure 3.4 Concrete Placement of RC Column (a) Mechanical Mixture, (b) Fresh Concrete (c) Formworks (d) Slump test (e) Compaction and (f) Constructed RC columns

3.6 Strengthening of RC Columns

After 28 days of curing, corner sides of hardened columns, except CA1 have been chipped off to get uneven surface. Afterward, angles were attached with corners of RC column with a cement mortar coating, as shown in Figure 3.5 (a). Cement mortar is used as a binding material between RC column surface and steel angle. When the mortar layer became dry, steel strips have been welded with angles at different spacing. One-fifth of the length of RC column, 300mm, from each end of the columns have less strip spacing than that of in the middle 900mm. It has been done to avoid failure at top and bottom of strengthened RC columns. Eleven strips were welded on each side of a RC column with a minimum welding length of 25mm to avoid shear failure at joints. Figure 3.5 (b) shows the strengthened RC columns after welding of steel strips with angles.



(a)



(b)

Figure 3.5 Steps of steel jacketing (a) Attachment of angle and (b) Welded Strips

3.7 Instrumentation and Testing of Jacketed Column

Test specimens have been tested when the concrete was over 120 days old. Columns have been placed vertically in Universal Testing Machine (Figure 3.6). The compressive load provided by a hydraulic jack capable of applying a maximum force of 2000 KN. The load was applied with a controlled displacement rate of 3 mm/min. Sample columns have been loaded monotonically until failure. To stay away from causalities full crushing has been avoided. To distribute the applied load uniformly on the top surface as well as to apply

eccentric load special type of cap for each column has been used. To apply eccentric load large diameter reinforcement has been welded at a certain distance measured from the center of the cross section on the top of the cap. Schematic diagram of typical cap is illustrated in Figure 3.7, where, e represents the eccentricity measured from the center of column and d represents the RC column's width as well as the internal dimension of steel cap. A steel plate has also been used at the bottom of test column during testing.



Figure 3.6 Universal Testing Machine (UTM)

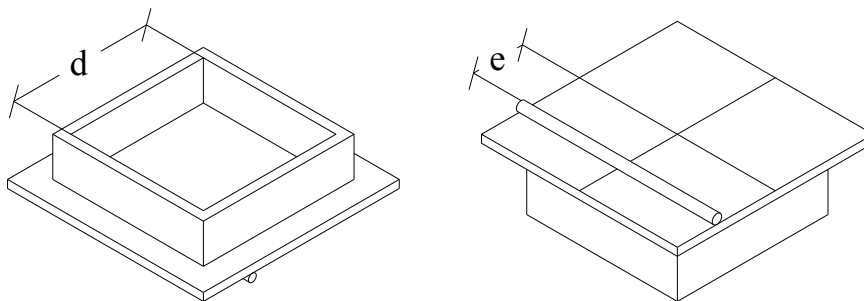


Figure 3.7 Schematic diagram of column cap used for eccentric loading

The specimen column CA1 and CA2 have been loaded concentrically, whereas CA3, CA4, and CA5 have been tested under eccentricity of 15, 37.5 and 67.5 mm representing an eccentricity to column width ratio (e/d) of 0.1, 0.25 and 0.45 respectively. Specimens have been tested using the test method of “Generic Compression Force vs. Deflection” using Horizon software, which records the applied displacement and resistance load automatically. Data acquisition has been done at every second during loading. Figure 3.8 through Figure 3.9 show un-strengthened and strengthened test columns before application of loads.

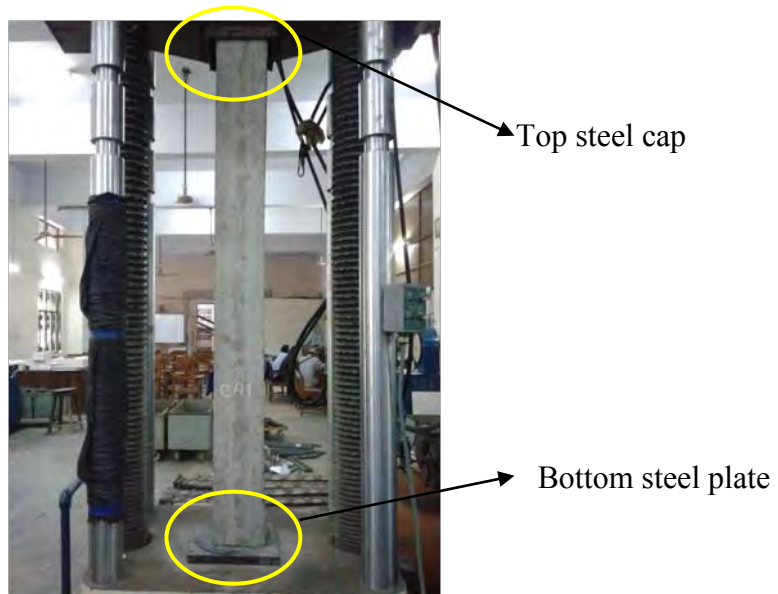


Figure 3.8 Un-strengthened RC column before loading

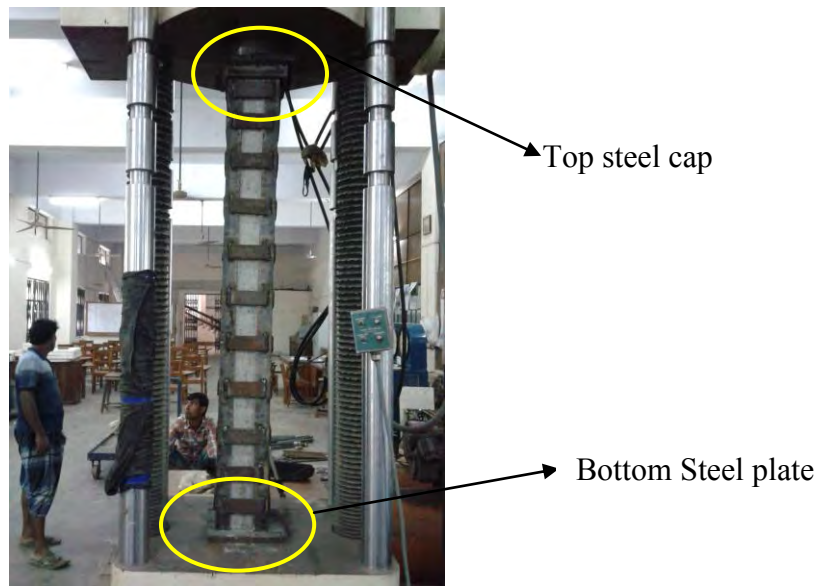


Figure 3.9 Strengthened RC column before loading

Test column CA6 has been tested horizontally as a beam using two points loading in the UTM. Figure 3.11 shows schematic diagram of the test setup with actual dimensions. In this case, as the machine displacement is not equal to the mid-span displacement of the specimen, displacement gauge (Figure 3.12) has been used to measure the specimen's mid span vertical displacement. Resistance load has been recorded by software associated with UTM.

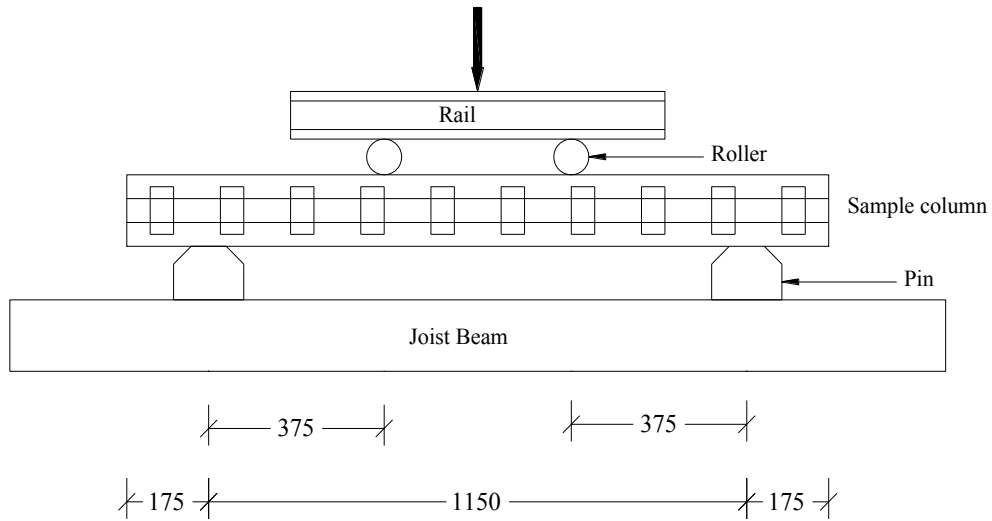


Figure 3.10 Schematic diagram of test setup for pure bending test

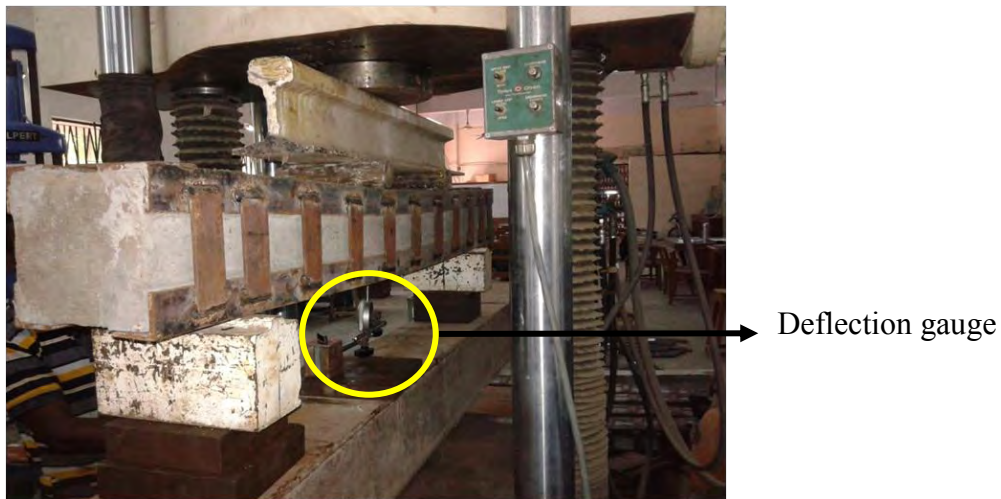


Figure 3.11 Setup for pure bending test of strengthened RC member

CHAPTER 4

FINITE ELEMENT MODELLING

4.1 Introduction

The objective of this chapter is to develop finite element model of steel angle and strip jacketed RC columns under different loading approach (i.e. concentric, eccentric etc.) and to simulate their behavior numerically with the test specimens of this study as described in the preceding chapter.

Basically, finite element simulation is necessary for scientific research because experimental works are both costly and time consuming. Though numerical simulation needs a deep insight of material and geometric behavior of structure however it reduces endeavor of experimental work. In this study, Graphical User Interface (GUI) of the finite element software ABAQUS/ Standard (HKS 2013) has been used. As constitutive component of jacketed RC columns concrete, steel angle, strip and reinforcement are modeled with different published material models, which will be discussed in the following sections. Some constraints have been defined in the FE models to simulate the interactions between different parts of jacketed RC columns. Newton-Raphson solution strategy is used to trace the behavior under controlled displacement type load up to failure.

This is followed by a detailed description of the geometry of finite element model, the material model parameters, the loading scheme and the end boundary conditions used to simulate the test columns.

4.2 Geometric Properties of the Finite Element Model

4.2.1 Element selection and mesh

The C3D8R elements (Figure 4.1 (a)) have been selected to model the concrete, steel angles and strips. The C3D8R element is an eight-node reduced integration brick element with

three translational degrees of freedom at each node. Three dimensional two-node truss elements designated as T3D2 (Figure 4.1 (b)) have been used to model the longitudinal and tie reinforcements.

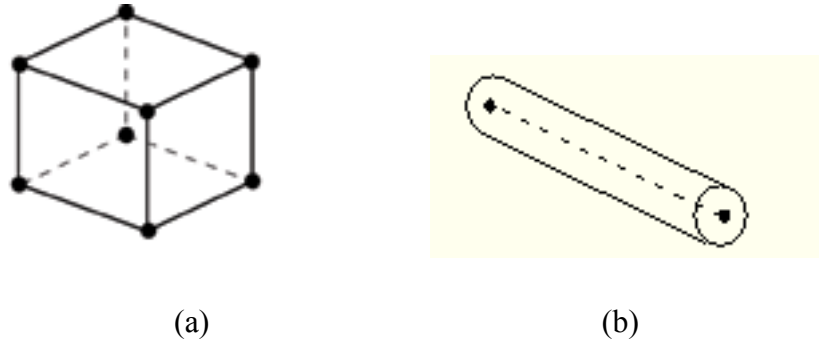


Figure 4.1 Finite elements used (a) C3D8R and (b) T3D2

Overall model has been meshed in a planned way. As the model has been done in GUI then the cross section of the RC column has been partitioned at the points where angles and long reinforcements are supposed to be in the same alignment. Then parts have been meshed with a maximum aspect ratio of 1.25. Since mesh sensitivity analysis has not been conducted in the present study, relatively small mesh sizes (25x25 mm and 25x20mm) have been selected to obtain accurate solution. A sample column after meshing has been presented in Figure 4.2.

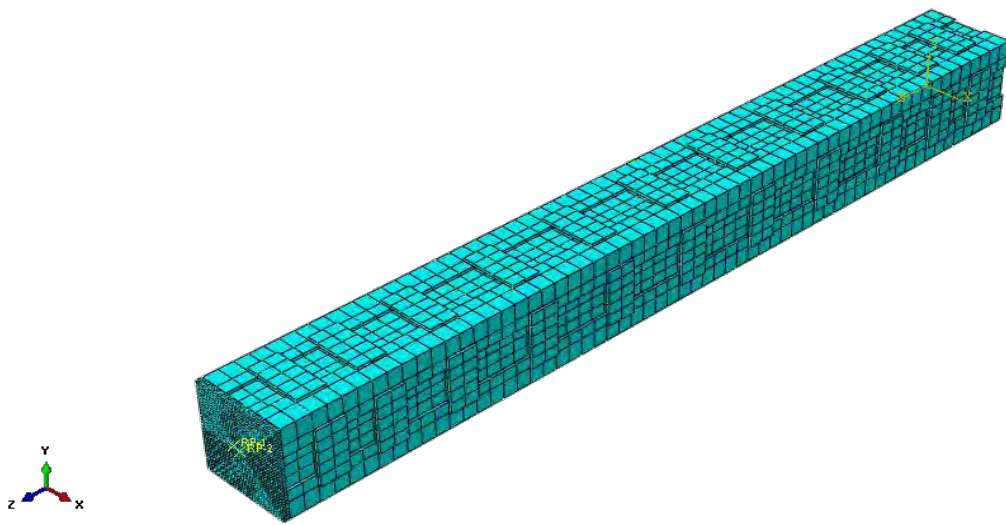


Figure 4.2 Mesh of steel angle and strip jacketed RC column

4.2.2 Interaction of different components

The jacketed RC column is a combination of different materials which are bonded to each other with different manners. Steel angles are bonded with concrete through a thin layer of cement mortar, whereas strips are welded with corner angles at a certain interval. To get the actual behavior of jacketed column in the FE model, it is necessary to define proper interaction among these contact surfaces. In Finite Element modeling connection of different parts can be idealized with some constraints, which eliminate degrees of freedom of a group of nodes and guide their motion to the motion of a master node(s).

Steel angle to concrete interaction

In the experimental study steel angles have been bonded with concrete throughout the length by cement mortar. To evaluate the properties of this bonded behavior no test has been done. Hard contact with normal and tangential properties has been applied as used by other researcher (Garzón Roca *et al.*, 2012). The “hard” contact relationship minimizes the penetration of the slave surface into the master surface at the constraint locations and does not allow the transfer of tensile stress across the interface. Concrete surface was assumed as master surface so that nodes of angle cannot penetrate into concrete elements.

Tangent behavior has been simulated with constant friction coefficient, μ . It is assumed to be 0.2 for Coulomb friction model. The basic concept of this model is to relate the maximum allowable frictional (shear) stress across an interface to the contact pressure between the contacting bodies. It assumes that friction coefficient is same in all directions (isotropic friction). For a three-dimensional simulation there are two orthogonal components of shear stress, τ_1 and τ_2 , along the interface between the two bodies. These components act in the slip directions for the contact surfaces or contact elements. ABAQUS combines the two shear stress components into an “equivalent shear stress”, τ , for the stick/slip calculations, where $\tau = \sqrt{\tau_1^2 + \tau_2^2}$. In addition, ABAQUS combines the two slip velocity components into an equivalent slip rate, $\gamma_{eq} = \sqrt{\gamma_1^2 + \gamma_2^2}$. The stick/slip calculations define a surface (Figure 4.3) in the contact pressure–shear stress space along which a point transitions from sticking to slipping.

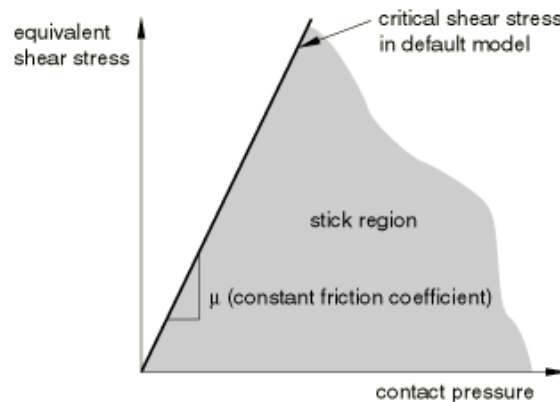


Figure 4.3 Qualitative shear stress vs. contact pressure relationship

Steel strip to steel angle interaction

In test specimens, steel strips were welded to the corner steel angles. As mentioned earlier welding lengths were sufficient to avoid shear failure at joints. To simulate this “tie” constraint was employed, where contact surface of angle and strip have been assumed as master and slave surface respectively.

Concrete to steel rigid plate interaction

Rigid plates have been modeled to distribute the applied displacement on the top of the jacketed column. Hard contact interaction properties with normal behavior have been assigned between bottom of the rigid plate and the top of the jacketed column. Bottom face of the rigid plate has been assumed as master surface because rigid surfaces are always should be defined as master surface.

Reinforcement to concrete interaction

To ensure bonding between the concrete and the reinforcing bars, the longitudinal and tie reinforcements were defined as “embedded” in the concrete, which effectively couple the behaviour of the rebar with the adjacent concrete mass. Nodal response of concrete element will be used to constrain the translational degrees of freedom of the embedded nodes (i.e., nodes of reinforcement elements).

4.2.3 End boundary conditions

The test columns were supported at the bottom on steel plate so that it cannot move horizontally and vertically. In the Finite Element model, similar types of boundary conditions have been applied at the end of the columns to restrain the translation of the bottom nodes of columns.

4.3 Material Properties used in the Finite Element Model

4.3.1 Concrete damage plasticity model

Concrete damage plasticity (CDP) model uses stress-strain relationship to define relative concrete damage. The model is a continuum, plasticity-based damage model for concrete (Lubliner *et al.*, 1989) that is capable of predicting both compressive and tensile behavior of the concrete material under low confining pressures. Compression hardening and tension stiffening models are used to define the complete behavior of concrete under loads. Therefore, CDP model in ABAQUS (HKS 2013) has been used to simulate the concrete material behavior in the steel angle and strip jacketed RC columns. In ABAQUS, stress-inelastic curves are input for this model, which are converted to stress-plastic strain curve automatically using damage variable. Qualitative stress strain curve for concrete material is presented in Figure 4.4. In addition to basic parameters that identify stress-strain relationships, parameters based upon the microstructure of concrete must also be identified. For this purposes dilation angle 15° has been incorporated in this finite element model.

Compressive behaviour

The complete compressive behavior can be divided into two portions. Initially, the linear elastic portion is defined using the modulus of elasticity in compression. The proportional limit or elastic limit for normal strength concrete is assumed to be 45% of its compressive strength. Later, the plastic regime i.e. the effective stress–strain curve (Figure 4.5) is developed using the function proposed by Carriera and Chu (1985) for uniaxial compression. The 28 days compressive stress-strain data has been used instead of test day data.

$$\frac{f_c'}{f_c} = \frac{\beta \frac{\varepsilon'}{\varepsilon_c}}{\beta - 1 + \frac{\varepsilon'}{\varepsilon_c}} \quad . . . \quad (4.1)$$

$$\beta = \frac{1}{1 - \frac{f_c'}{E\varepsilon_c}} \quad . \quad (4.2)$$

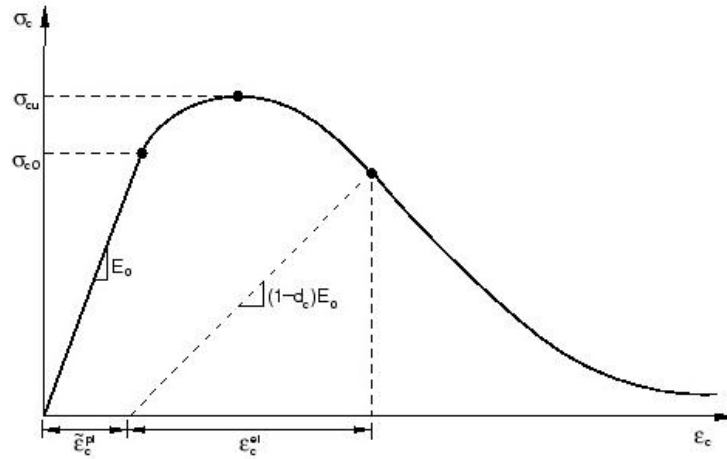
$$\varepsilon_c' = (0.2 f_{cu}' + 13.06) \times 10^{-4} \quad (4.3)$$

Here β is a material parameter which depends on the shape of the stress- strain diagram. A value of $\beta = 2$ has been used in this study which is proposed by Tulin and Grestle (1964). Concrete strain is measured by using equation 4.3 as prescribed by Almusallam & Alsayed, 1995.

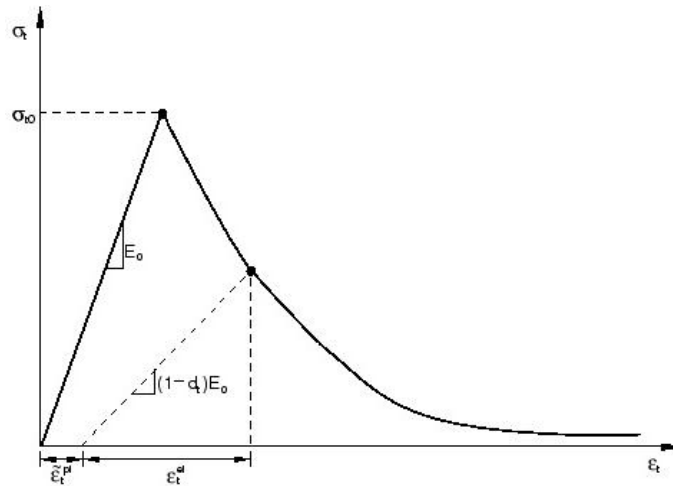
The uniaxial compression hardening curve is defined in terms of the inelastic strain, $\varepsilon_c^{\sim\text{in}}$, which is calculated using equation 4.4. The damage plasticity model automatically calculates the compressive plastic strains, $\varepsilon_c^{\sim\text{pl}}$ using equation 4.5, using a damage parameter, d_c , that represents the degradation of the elastic stiffness of the material in compression.

$$\varepsilon_c^{\sim\text{in}} = \varepsilon_c - \frac{f_c}{E_c} \quad (4.4)$$

$$\varepsilon_c^{\sim\text{pl}} = \varepsilon_c^{\sim\text{pl}} - \frac{d_c f_c}{(1-d_c)E_c} \quad (4.5)$$



(a)



(b)

Figure 4.4 Qualitative response of concrete to (a) Compression and (b) Tension

Tensile behaviour

The uniaxial tensile strength of concrete, f'_t , is assumed to be 10% of the uniaxial compressive strength, f'_c , for the normal strength concrete as observed by Marzouk and Chen (1995). Concrete tension properties for damage model are defined in two stages: the linear elastic portion up to the tensile strength and the nonlinear post peak portion which is called the tension stiffening. The first part is defined using the modulus of elasticity of concrete (E_c) and the yield stress of concrete in tension. After peak point, strain softening

represents the response of the cracked concrete that is expressed by a stress versus cracking strain curve. A same form of serpentine curve (Equation 4.1), as used to predict the compressive behaviour, is used for the average stress- inelastic strain diagram of reinforced concrete in tension, f_t is taken as 10% of f_c . Response of concrete under tension is presented in Figure 4.6.

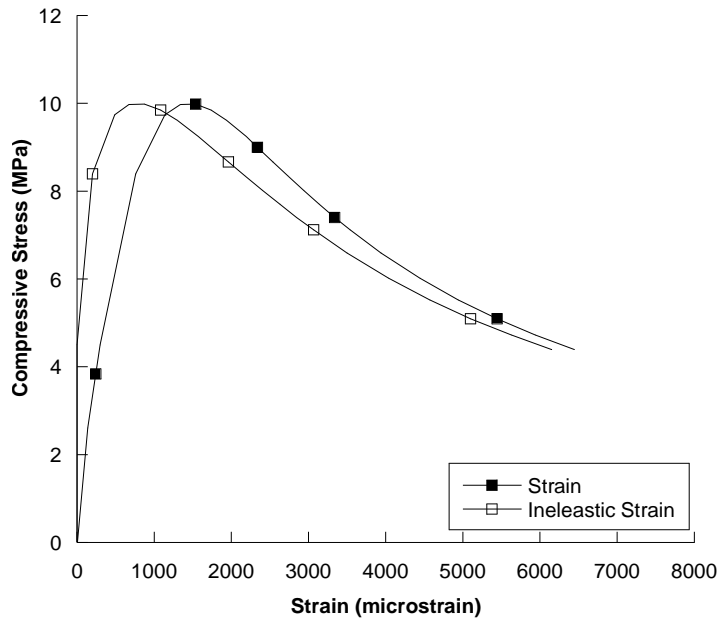


Figure 4.5 Compressive stress strain curve for concrete

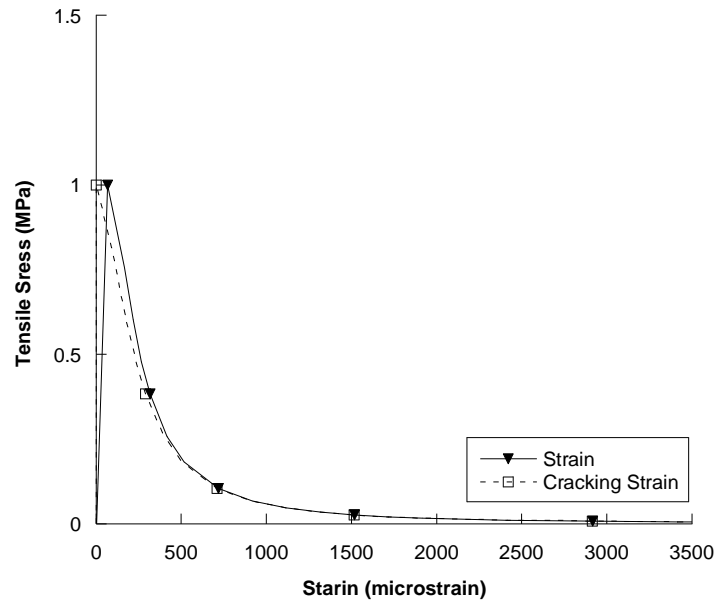


Figure 4.6 Tensile stress strain curve for concrete

4.3.2 Verification of concrete model

As concrete is highly complex in behavior it is necessary to verify the CDP model with test specimen concrete properties. Initial verification has been done by comparing the stress-strain curve of a cylinder, modeled (Figure 4.7) in ABAQUS with the experimental stress strain curve at 28 day. The cylinder has a dimension of 100x200mm. Stress-strain curve shows a good agreement with the experimental behavior (Figure 4.8).



Figure 4.7 Finite element model of Concrete cylinder

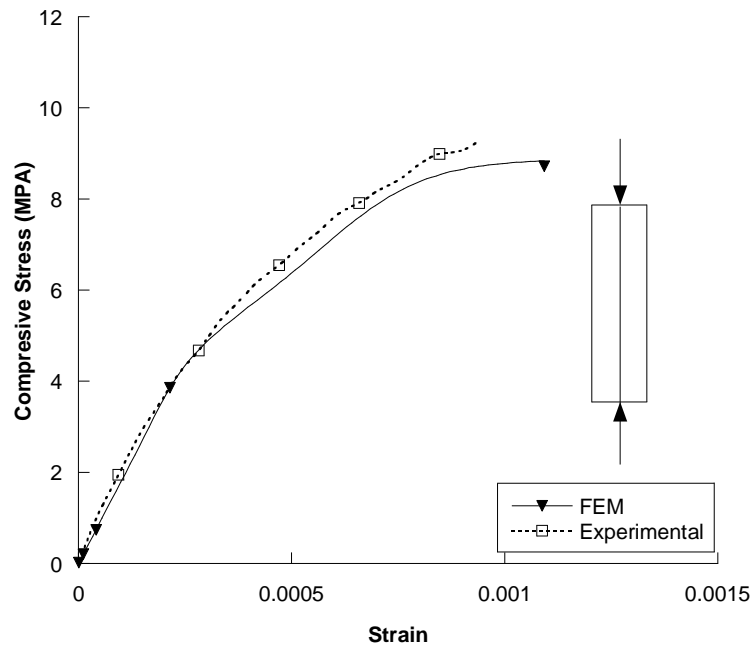


Figure 4.8 Stress-strain curve of cylinder under compression

4.3.3 Material model of steel

Steel is a ductile material which experiences large inelastic strain beyond the yield point. So, the true stress and logarithmic strain graph which is also called hardening curve, as shown in Figure 4.9, is considered for modeling the material behavior of steel. It's a bilinear curve showing variation of true stress with plastic strain.

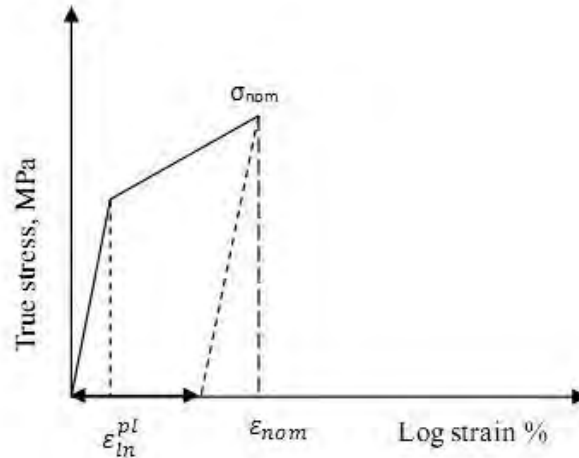


Figure 4.9 Qualitative stress strain curve of steel

If nominal stress-strain data for a uniaxial test is available and the material is isotropic, a simple conversion (Lubliner *et al.*, 1990) to true stress and logarithmic plastic strain is as follows-

$$\sigma_{true} = \sigma_{nom}(1 + \epsilon_{nom}) \quad (4.6)$$

$$\epsilon_{ln}^{pl} = \ln(1 + \epsilon_{nom}) - \frac{\sigma_{true}}{E} \quad (4.7)$$

Where, E is the Young's modulus of the material.

ABAQUS (HKS 2013) Standard needs two data points consisting of stress strain values along with the modulus of elasticity and Poisson's ratio. The two data points are the stress and equivalent plastic strain at points representing start of yielding and ultimate point. The Poisson's ratio for steel is considered to be 0.3. Figure 4.10 through Figure 4.13 show the

bilinear representation of steel angles, strips, 10mm diameter and 8mm diameter reinforcements respectively.

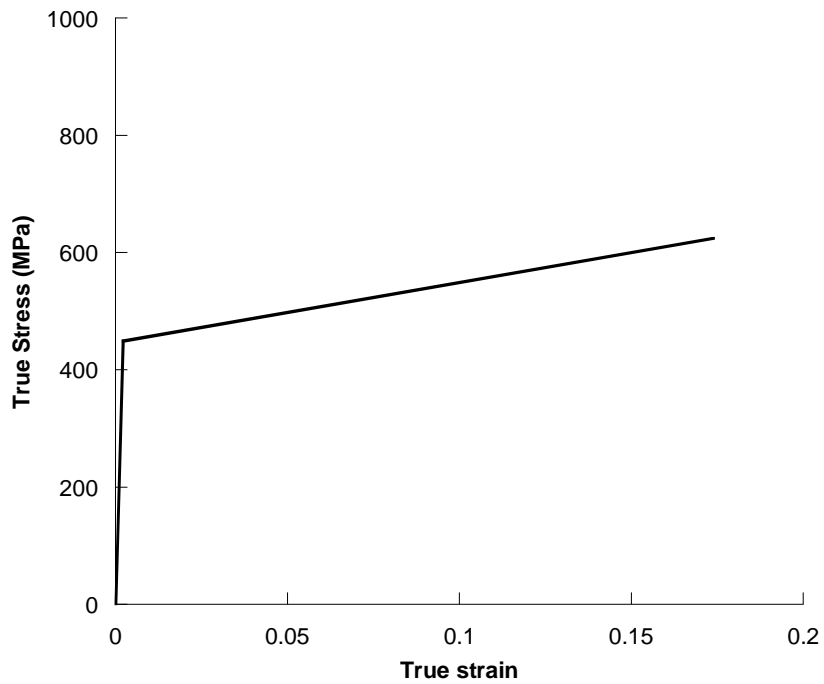


Figure 4.10 Bilinear stress strain curve of Steel Angles

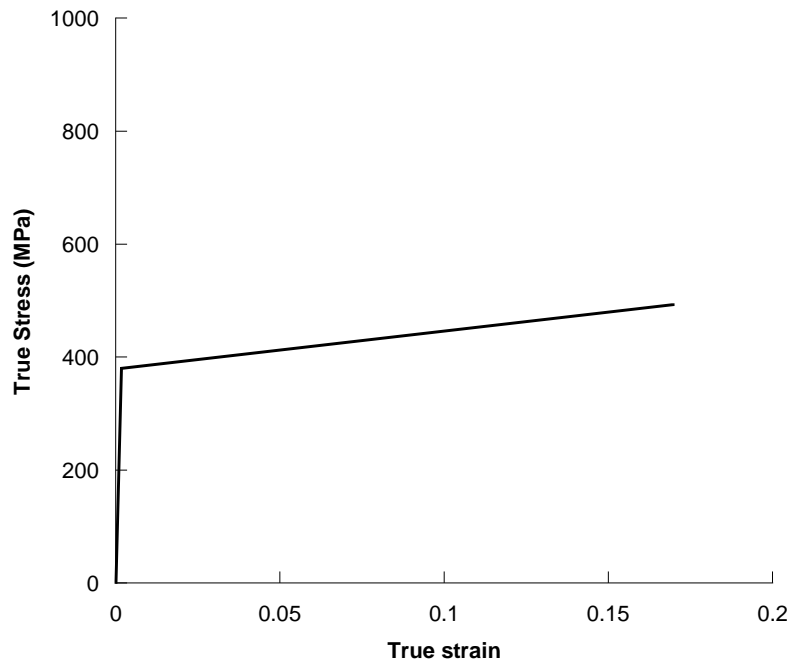


Figure 4.11 Bilinear stress strain curve of Steel Strips

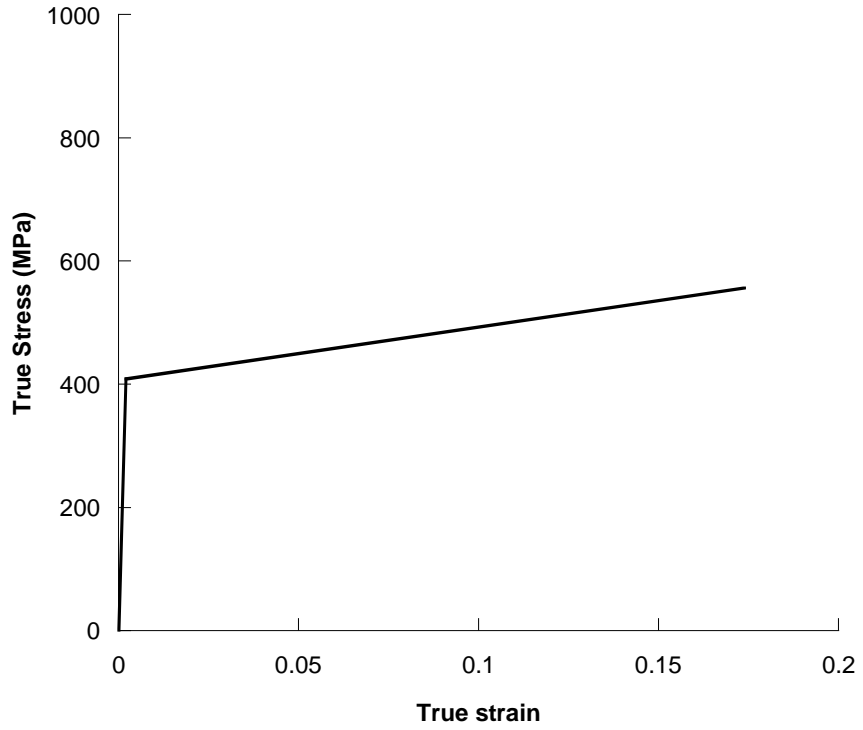


Figure 4.12 Bilinear stress strain curve of 10mm diameter reinforcement

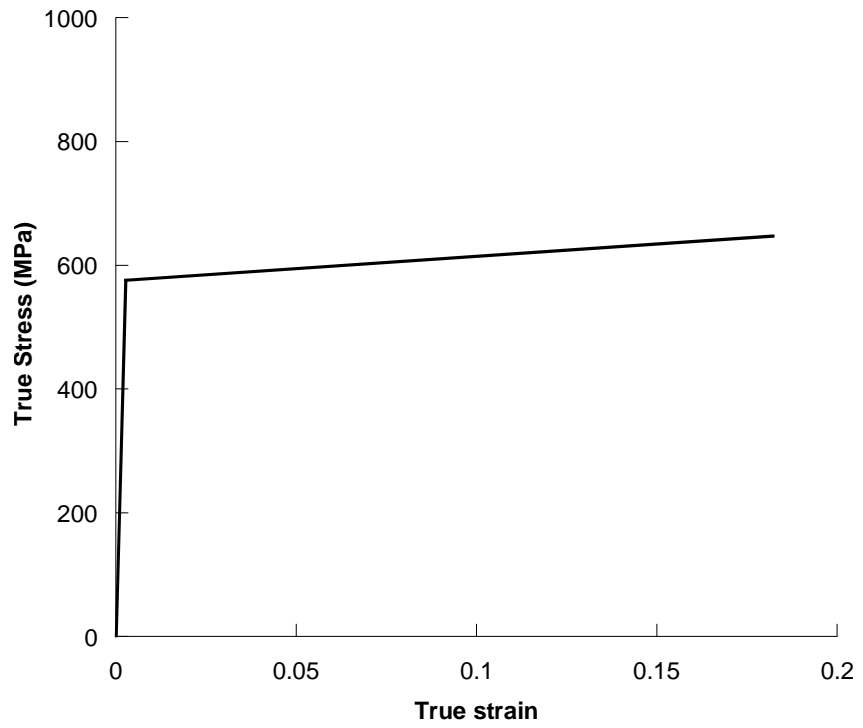


Figure 4.13 Bilinear stress strain curve of 8mm diameter reinforcement

4.4 Load Application and Solution Strategy

4.4.1 Application of load

Loads can be applied in two approaches namely force and displacement controlled. In this study displacement control approach has been selected as it has more scope to predict the nonlinear behaviour. Controlled displacement has been applied monotonically on some selected points depending on the loading criteria (i.e. concentric or eccentric loading). The displacement load was applied to the reference point of the rigid body, which coincides with the center of the line of load application in the tests. In the case of concentric load reference point coincide with the center of the cross section of the test column. For the eccentrically loaded columns the loading reference points were defined at a certain distance (i.e. eccentricity, e) measured from the center of the cross section of the column.

4.4.2 Solution strategy

Newton-Raphson solution strategy is implemented in the finite element models to obtain solution for this nonlinear problem. In a nonlinear analysis the solution usually cannot be calculated by solving a single system of equations, as would be done in a linear problem. Instead, the solution is found by applying the specified loads gradually and incrementally working toward the final solution, which is called iterative process. Therefore, in the analysis the simulation is broken into a number of load increments and the approximate equilibrium configuration at the end of each load increment is formulated. It often takes several iterations to determine an acceptable solution to a given load increment. The sum of all of the incremental responses is the approximate solution for the nonlinear analysis. Thus, the incremental and iterative procedures are combined for solving nonlinear problems.

Any nonlinear equation can be written as

$$f(x) = 0 \tag{4.8}$$

Where, x is the solution to be calculated.

Considering a point close to the solution x and assuming the function to be smooth enough near the solution, the above equation can be written as a truncated Taylor series expansion approximately as

$$f(a) + f'(a)\Delta x = 0 \quad (4.9)$$

The above equation forms the basis for the iterative procedure to calculate the solution. Assuming an initial guess x_n for the solution is known, the increment Δx to be added to this approximation to get an improved value for the solution which is calculated as

$$\Delta x = -\frac{f(x_n)}{f'(x_n)} \quad (4.10)$$

The improved approximation after this first iteration is then obtained as

$$x_{n+1} = x_n + \Delta x \quad (4.11)$$

$$x_{n+1} = x_n - \frac{f(x_n)}{f'(x_n)} \quad (4.12)$$

The iteration is repeated until the increment Δx is smaller than a pre-defined tolerance. The more the iteration runs the more Δx approaches zero or tolerance if it is a continuous function. Figure 4.14 shows the schematic representation of the Newton-Raphson method showing the iteration from the initial guess x_n to the next approximation x_{n+1} to the value zero of a function $f(x)$.

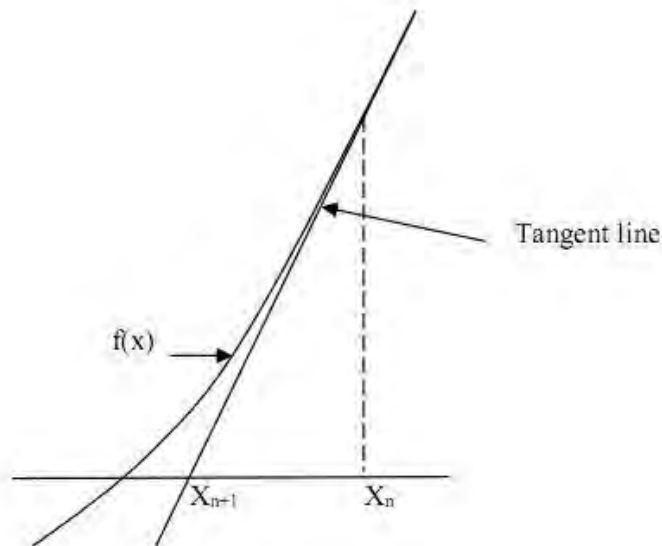


Figure 4.14 Newton-Raphson solution strategy

5.1 General

In this study, an experimental program has been designed to investigate the performance of the steel angle and strip jacketed RC columns under various load eccentricities. One specimen has also been tested as a beam under pure flexure i.e. two point loading. Effect of eccentricity on the capacities of steel jacketed RC columns and performances of jacketing method under eccentric loads have been checked experimentally by comparing axial load–displacement behavior with that of an un-strengthened RC column. Moreover, experimental load-moment interaction diagram of steel jacketed RC column has also been compared to the RC column’s nominal interaction diagram to check the enhancement of safety margin in the load-moment domain.

Further effort has been given to model un-strengthened and strengthened RC columns in Finite Element Program (ABAQUS). Accuracy of the model has been checked by comparing ultimate capacities with the experimental capacities. Numerical simulation of steel jacketed RC column facilitates to conclude more information about the relative contribution and confinement of RC core column, mid-height displacement, and efficiency of steel jacketed RC columns under eccentricity etc.

Many researchers proposed analytical models to predict axial capacity and interaction diagram of steel angle and strip jacketed columns. This study also intends to validate the analytical models available in literature. All the above mentioned performance checks and effect evaluations are presented with particular details in the following sections. To do this both experimental and FEM results have been used simultaneously.

5.2 Experimental Results

5.2.1 Load deflection responses

In this study column CA1 and CA2 have been constructed as un-strengthened and strengthened RC columns. Figure 5.1 shows the axial load displacement curves of un-strengthened (CA1) and strengthened (CA2) RC columns. Strengthened RC column shows much higher strength and ductility than the un-strengthened RC column. After reaching ultimate load capacity un-strengthened RC column shows sharp post peak decline whereas steel jacketed RC column shows gradual post peak decline with a higher axial displacement.

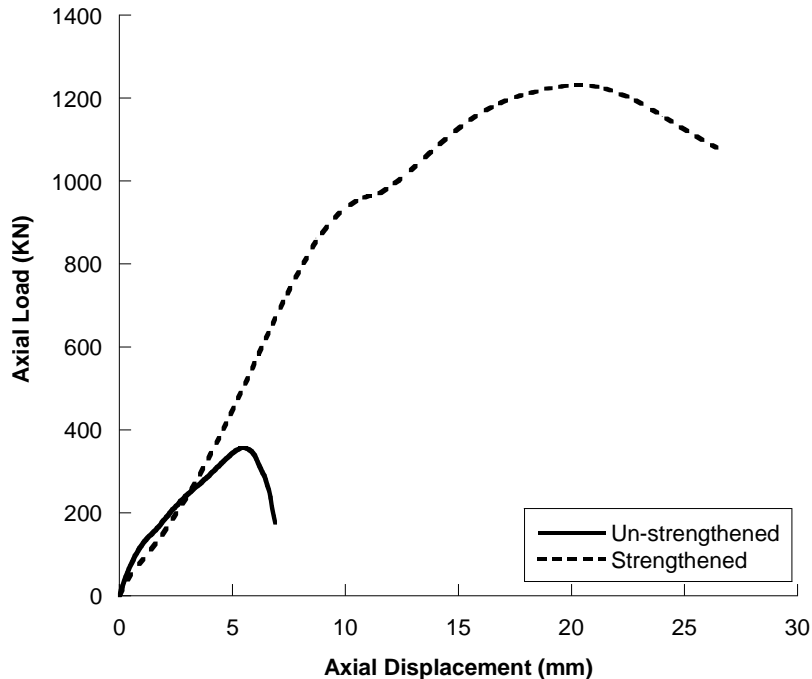


Figure 5.1 Axial Load-Displacement curves of un-strengthened and strengthened RC columns

Figure 5.2 shows load displacement curves of four strengthened RC columns subjected to different eccentricities. In this study, column CA2, CA3, CA4, and CA5 have been tested with load eccentricities of 0, 15, 37.5, and 67.5 mm respectively measured from the center of column cross section. The angle and strip configurations have been kept similar. It is

evident, from the load versus displacement curves that increase of eccentricity results in a lower initial stiffness. This can be attributed to the combined stresses of axial and bending moment, which induce large deflection with less axial loads. It has been observed that all the jacketed RC columns show an approximate yield point like steel. This may happen due to the direct loading of angle sections which carries most of the applied loads. It has been found from finite element analysis that angle sections carry about 62% of the total load at ultimate point. The yield point of sample column shifted to the right with the increase of eccentricity. Further observations from experimental program in terms of axial capacity and displacement ductility are presented in the following section.

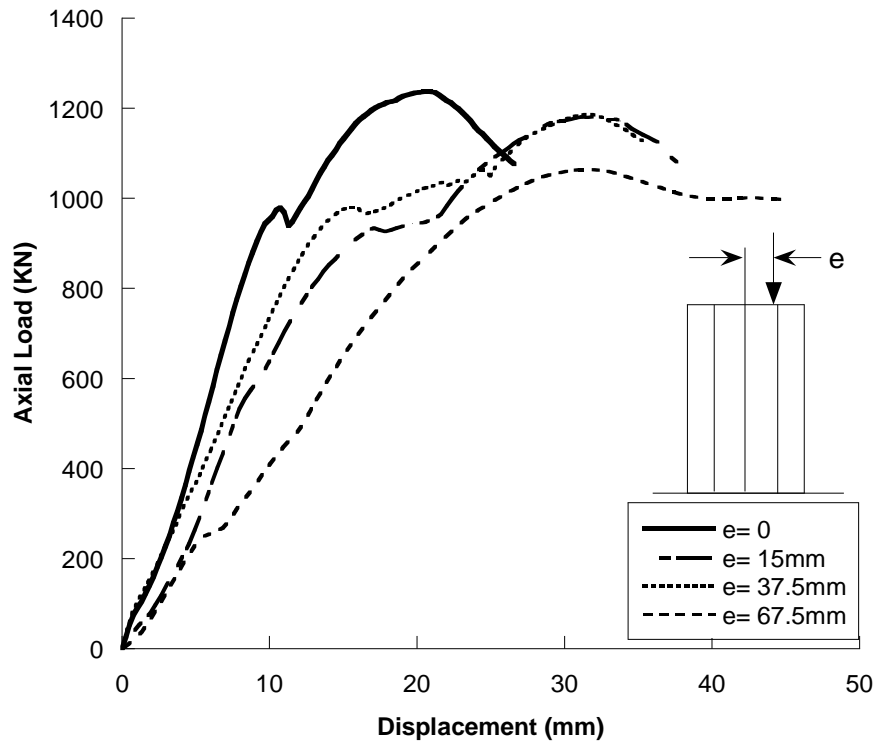


Figure 5.2 Axial Force-Displacement graphs of jacketed columns with different load eccentricity

5.2.2 Axial load capacity and displacement ductility

Table 5.1 presents the experimental ultimate load capacities of the test columns. In case of the concentric loading, it has been found that strengthening of RC column using steel angle and strip results in about 240% increase in the axial capacities of the RC column. This is certainly a good achievement of this jacketing method. However, presence of load

eccentricity can reduce this enhancement by inducing more compressive stress on the cross section of column compared to concentric loading due to the presence of both axial and bending stress simultaneously. So, presence of eccentricity leads to lower axial capacity compared to concentrically loaded column which is evident in Figure 5.2. The strengthened RC columns' capacity reduces 15% compared to the concentric loading as the load eccentricity to column width ratio rises from 0 to 0.45. It is clear from Figure 5.3 that the reduction trend of ultimate load capacity of strengthened RC column with the increase of eccentricity is approximately linear. From this study it can be summarized that eccentricity itself reduces the axial capacity of jacketed RC columns.

Table 5.1: Ultimate load capacities of test columns

Sample	Strengthening condition	Eccentricity Ratio (e/d)	Ultimate capacity (KN)	Displacement at ultimate capacity (mm)	Displacement ductility
CA1	Un-strengthened	0	360	5.6	1.30
CA2	Strengthened	0	1235	20.8	1.55
CA3	Strengthened	0.10	1180	32.1	1.43
CA4	Strengthened	0.25	1185	31.8	1.60
CA5	Strengthened	0.45	1065	32.0	1.62

In RC columns, the strength degradation is partially caused by crushing of the concrete core accompanied by the buckling of the longitudinal bars, which is also found in this study. However, presence of strips with angles prevents buckling of the longitudinal bars. Failure is initiated by buckling of the compression steel angles in between strips followed by concrete crushing. The failure of steel jacketed RC column occurs with a large axial shortening compared to un-strengthened RC column, which indicates more ductile behavior. This is also reported by Campione (2013) based on experimental investigation.

Ductility of the column can be investigated from displacement ductility index. Displacement ductility can be defined as the ratio of the displacement at ultimate load to the displacement at 85 percent of the ultimate load. Displacement ductility values of all test columns are presented in Table 5.1. Concentrically loaded strengthened RC columns shows relatively more displacement ductility compared to un-strengthened RC column, which is about 19% in this study. However, when eccentricity to column width ratio changes from 0 to 0.45 the displacement ductility of strengthened RC column increases about 4%.

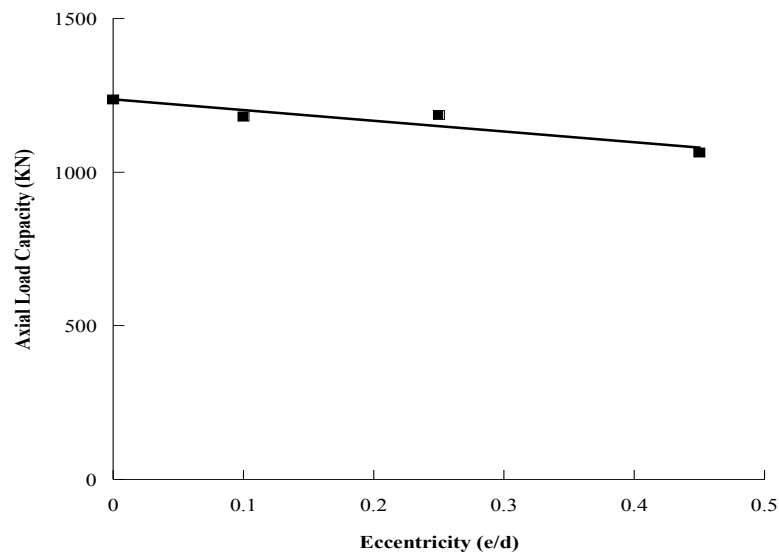


Figure 5.3 Effect of eccentricity on axial load capacity

5.2.3 Failure modes

Un-strengthened RC column (CA1)

Figure 5.4 shows overall failure mode of RC column under concentric loads. Figure 5.5 and Figure 5.6 show close views of the reinforcement and concrete failure respectively. As mentioned earlier failure of RC columns initiated with the crushing of concrete followed by buckling of longitudinal reinforcements.



Figure 5.4 Failure mode of un-strengthened RC column under concentric loads



Figure 5.5 Buckling of longitudinal reinforcements in un-strengthened RC column under concentric loads



Figure 5.6 (a) Top concrete crushing and (b) Bottom concrete crack of un-strengthened RC column under concentric loads

Strengthened RC column under concentric load (CA2)

Figure 5.7 and Figure 5.8 show the failure modes of strengthened RC column under concentric loads. The failure is initiated by local buckling of the steel angles at the top and bottom ends. The local buckling is also observed in between two consecutive strips i.e. 3rd and 4th strips from top. After local buckling, slight concrete cover spalling occurred followed by crushing of concrete. No buckling of the longitudinal rebars is observed during the test at the failure point.



Figure 5.7 Steel angles buckling at (a) Top and (b) Bottom of strengthened RC column under concentric loads



Figure 5.8 Concrete splitting of strengthened RC column at bottom under concentric loads

Strengthened RC column under 15mm eccentric load (CA3)

Figure 5.9 and Figure 5.10 show failure modes of strengthened RC column under 15 mm eccentric loads. In this column, local buckling observed in between 3rd and 4th strips from the top end of column. This is followed by concrete cover spalling. In this column, overall buckling of the column is also observed at failure. This is due to the bending moment resulting from the eccentricity of the applied load.



Figure 5.9 Failure mode of strengthened RC column with eccentricity of 15mm



Figure 5.10 Buckling of steel angles and concrete crushing in between strips with eccentricity of 15mm

Strengthened RC column under 37.5 mm eccentric load (CA4)

Figure 5.11 through Figure 5.13 show the failure modes of strengthened RC column under 37.5 mm eccentricity. In this column, failure of the weld joint between the strip and steel angle joint near top is observed followed by crushing of concrete near top region of the column. Local buckling of the steel angles at the compression side between 3rd and 4th strips from top is also observed. The global buckling of specimen is also evident with a single curvature.

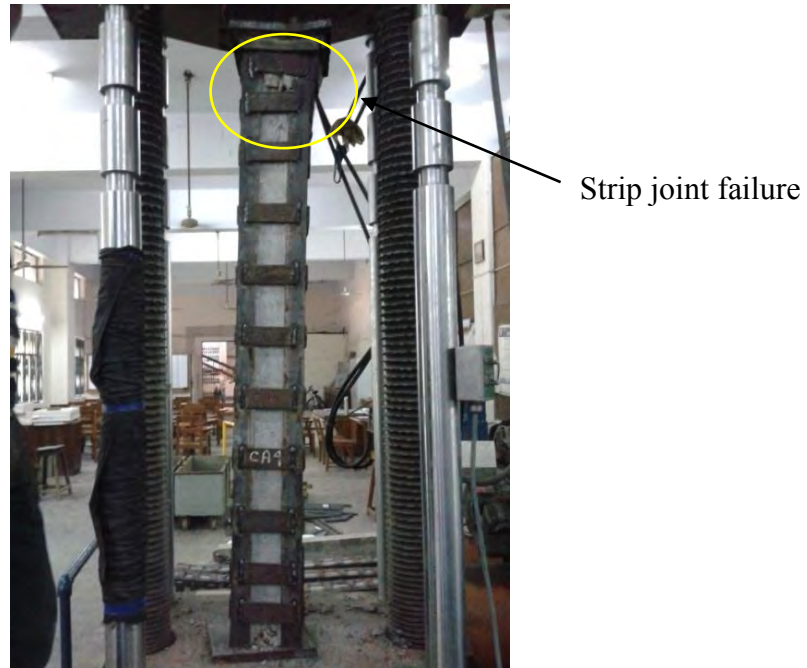


Figure 5.11 Failure mode of strengthened RC column with eccentricity of 37.5 mm



Figure 5.12 Buckling of steel angles and concrete spalling in between strips with an eccentricity of 37.5mm



Figure 5.13 Buckling of compression side steel angles at top with an eccentricity of 37.5 mm

Strengthened RC column under 67.5 mm eccentric load (CA5)

Figure 5.14 and Figure 5.15 show the failure modes of strengthened RC column under 67.5 mm eccentricity. The failure is initiated with the buckling of steel angle at compression side followed by large amount of concrete spalling at the location of local buckling. Global buckling of the column is also observed with double curvature.

Strengthened RC column under pure bending (CA6)

Figure 5.16 shows the steel angle and strip jacketed RC column subjected to two point loading. The failure of the specimen under two point loading initiated with shear crack near supports with a load of half its bending capacity. Flexural cracks appeared in the bottom face of the specimen near to the capacity. However, the concrete crushing and cracks at top and bottom were minor.

From the above discussion, it is evident that the failure of steel angle and strip jacketed RC columns initiated with local buckling of the steel angles followed by concrete cover spalling and concrete crushing irrespective to eccentricity. However, eccentricity changes the overall buckling shape. Deformed shape changes from single to double curvature as the eccentricity ratio rises from 0.1 to 0.45.



Figure 5.14 Failure mode of strengthened RC column with an eccentricity of 67.5 mm



Figure 5.15 Buckling of steel angles and concrete crushing in between strips with eccentricity of 67.5mm



(a)

(b)

Figure 5.16 Failure modes (a) overall deflected shape and (b) shear crack of Steel jacketed RC column under pure bending

5.2.4 Load-Moment interaction of steel angles and strips jacketed RC column

To develop the failure envelope, also known as interaction diagram of the jacketed RC column five jacketed square RC columns have been tested with different eccentricities. Four columns have been tested vertically as column whereas one sample has been tested horizontally as beam under two point loading for pure bending capacity. Figure 5.17 shows approximate failure envelope for 150x150 mm RC square column jacketed with 50x50x5 mm angles at corners and 125x50 mm strips at an interval of 150mm. Figure 5.17 also shows the nominal load-moment interaction diagram obtained from SAP 2000 section designer module using strain compatibility method for un-strengthened RC column. Comparing two failure envelopes it can be concluded that within the scope of this study steel angle and strip jacketing scheme is highly effective to upgrade the safety margin of column for both eccentric and concentric loading.

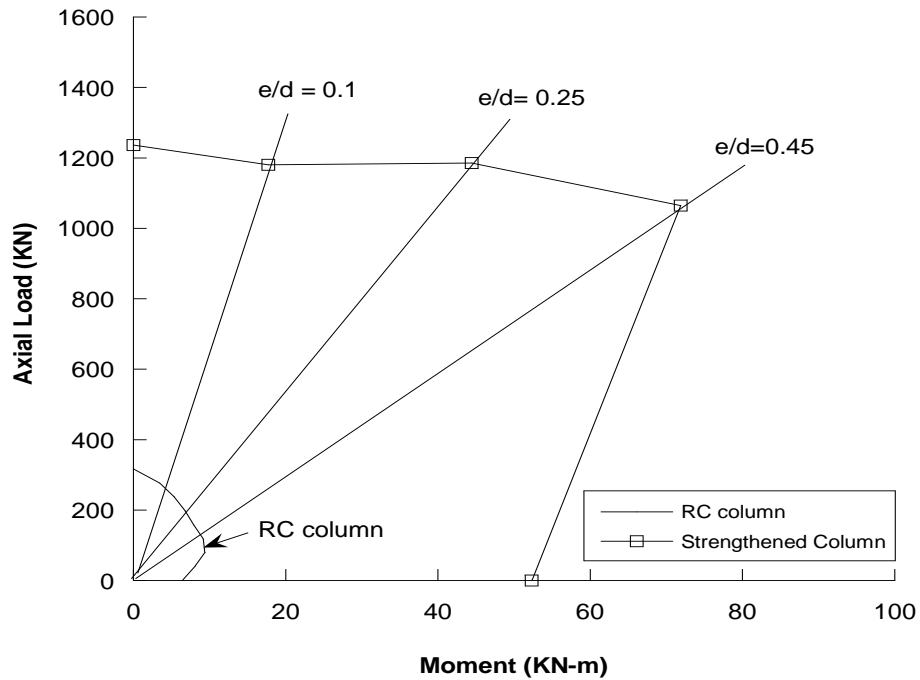


Figure 5.17 Interaction Diagram of RC column with and without jacketing

5.3 Performance of Finite Element Model

5.3.1 Initial model verification

In order to validate the finite element models, a comparison between the experimental and finite element results has been carried out. It has been determined first whether the ultimate load obtained numerically (P_{FEM}) matched the ultimate load obtained in the experimental study (P_{Exp}). Then the failure modes were checked with the experimental study.

Table 5.2 presents ultimate load capacities of finite element models along with experimental results. Considering all finite element models of this study, it can be concluded that FE models overestimated the experimentally obtained load capacities by a maximum of 9%. This can be attributed to the variability in concrete strength and bonding imperfection that might have been occurred during the test. However, the mean of experimental to numerical capacity ratio is 0.94, with a standard deviation of 0.04, which indicates a good agreement with experimental results.

Table 5.2: Ultimate load capacities of finite element models

Test column	Strengthening condition	Eccentricity (e/d)	Ultimate capacity		P_{EXP}/P_{FEM}
			Experimental (KN)	FEM (KN)	
CA2	Strengthened	0	1235	1235	1.00
CA3	Strengthened	0.10	1180	1250	0.94
CA4	Strengthened	0.25	1185	1305	0.91
CA5	Strengthened	0.45	1065	1165	0.91
Mean					0.94
Standard deviation					0.04

The failure mode of strengthened RC column observed in the finite element analysis is compared to that observed in the experiment. Figure 5.18 shows the buckling of the compression side steel angle between two strips as found in the finite element analysis. Similar behavior was observed in the test. Moreover, maximum stresses on the compression side steel angles have been extracted from finite element analysis. The maximum stress of compression angles at the ultimate load is about 512 to 528 MPa. This stress level is greater than the yield strength (450 MPa) and found to be less than ultimate strength (624 MPa) of angle material. It is worth to mention that, this stress level is more than the Euler elastic buckling strength of steel angles, calculated as 208 MPa. This stress analysis indicates the occurrence of inelastic buckling of angles.

From these comparison of axial capacities and failure modes it can be concluded that finite element models can predict the actual behavior of steel angle and strip jacketed RC columns. The finite element model has been further used to explain the behavior of jacketed columns under eccentric loads in the following sections, which is the main concern of this study.

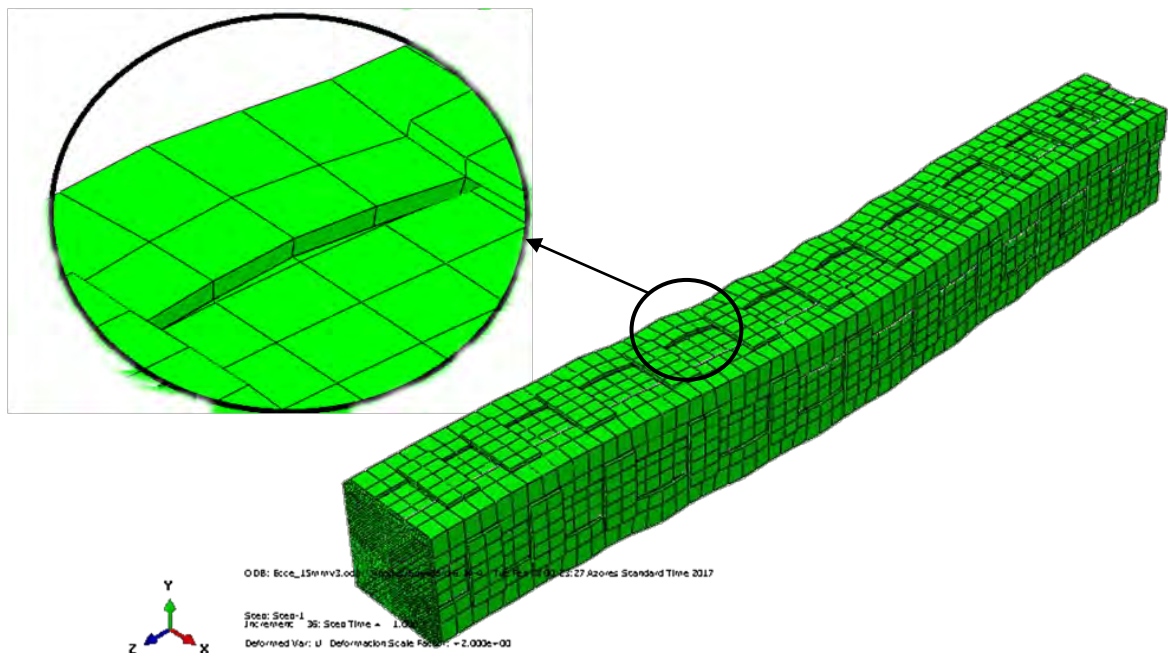


Figure 5.18 Deformed shape of the strengthened RC column with load eccentricity of 15 mm

5.3.2 Efficiency of strengthening

Efficiency of strengthening method under eccentricities is measured by comparing the ultimate capacities of FE models of un-strengthened and strengthened RC columns under same load eccentricities. Table 5.3 shows ultimate capacities of un-strengthened and strengthened RC columns under various eccentricities. It is evident that the efficiency of steel angle and strip jacketing method to upgrade the load capacities of RC columns increases as the eccentricity rises. In this study, under lower eccentricity ($e/d = 0.1$) strengthened RC column shows 330% capacity increase compared to the un-strengthened RC column subjected to same levels of load eccentricity. On the other hand, in case of higher eccentricity ($e/d = 0.45$) the capacity of strengthened column increases 850% compared to corresponding un-strengthened RC column. It indicates that this jacketing method can easily be applied in RC columns strengthening where accidental eccentricity is very common.

Table 5.3: Efficiency of steel angle and strip jacketing method

Eccentricity ratio, (e/d)	Axial capacity (KN)		Capacity increase (%)
	RC column	Strengthened column	
0	285	1235	330
0.15	182	1250	585
0.25	187	1305	600
0.45	122	1165	850

5.3.3 Concrete confinement

In steel angle and strip strengthened RC columns, as compressive stress of concrete approaches to the uniaxial compressive strength, lateral strains become very high due to progressive cracking. After the dilation of concrete, strips come into action which leads the concrete to take more load in nonlinear stage by confinement which delays the failure.

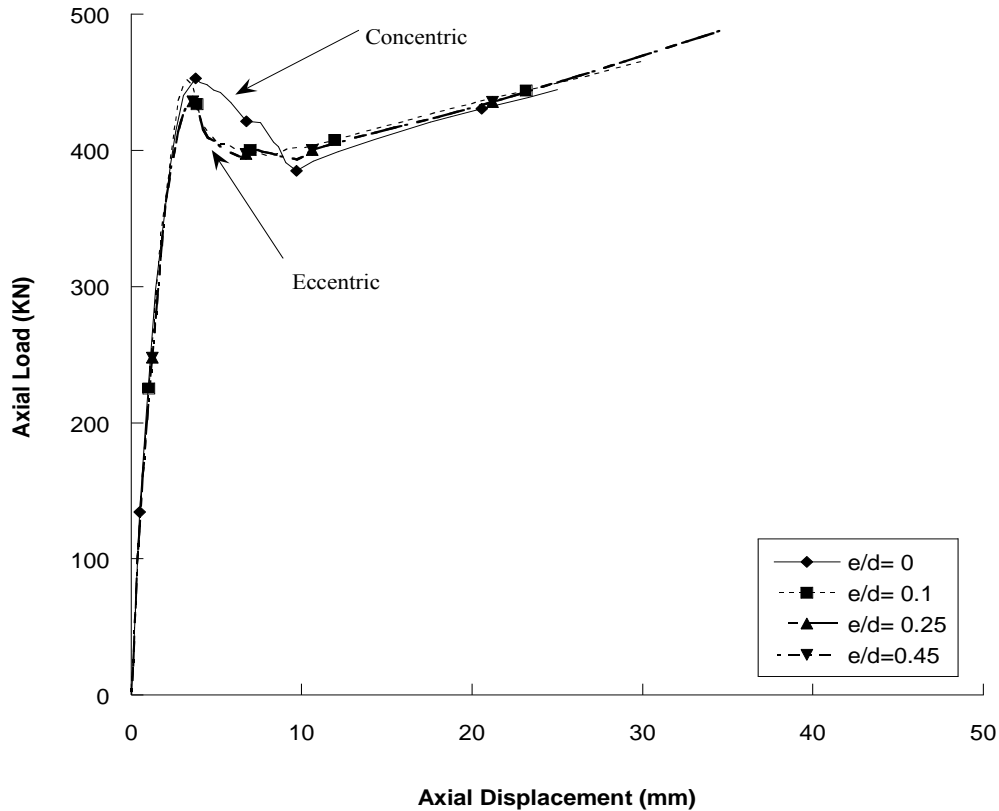
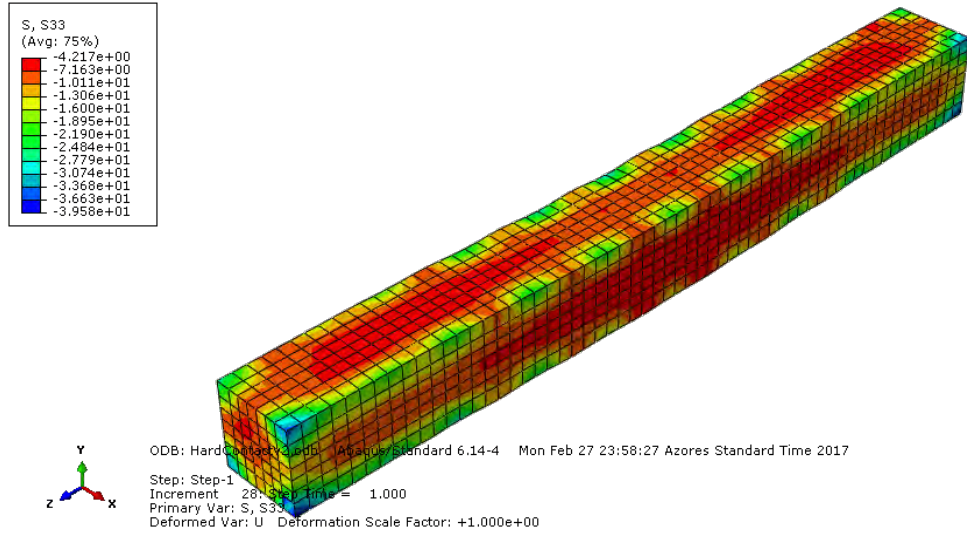


Figure 5.19 Axial load carried by RC core for different eccentricities

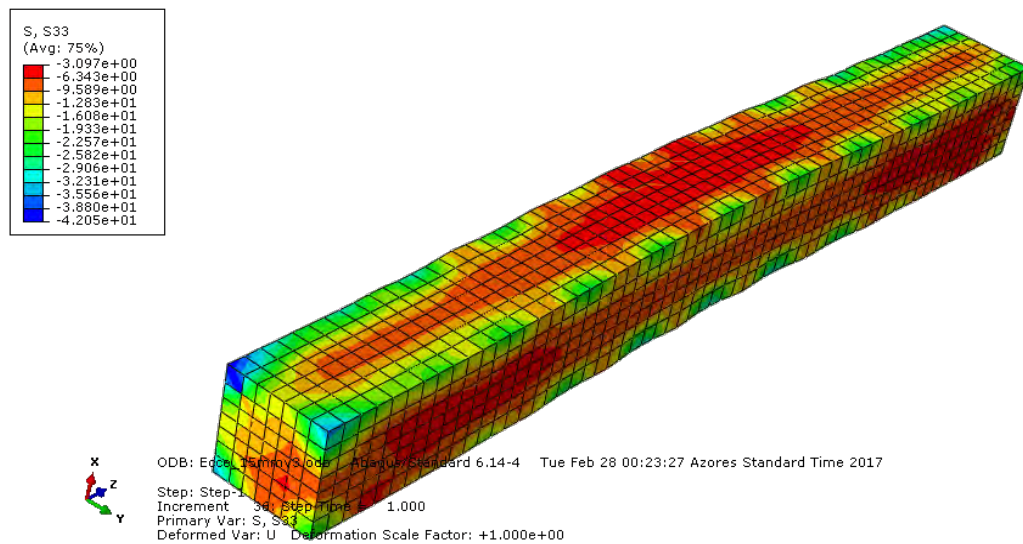
Figure 5.19 shows the load carried by only RC core at ultimate capacity for various load eccentricities. From this figure, it is evident that the softening behavior of concrete differs from concentric to eccentric loading. Load-displacement softening branch of concentrically loaded jacketed RC column is more prolonged than the eccentrically loaded columns. In case of eccentric loading the strain hardening of concrete started at early displacement compared to concentric loaded jacketed RC column, which indicates the early activation of confinement by external steel cage.

Figure 5.20 shows concrete stresses for sample columns with eccentricities of 0 and 15mm at ultimate capacity. It is evident that external steel cage comes into action and shows stresses more than the plain concrete, which was found 10MPa from laboratory test. Figure 5.21 and Figure 5.22 show an increasing trend of confined concrete stress and RC

core's contribution as the eccentricity rises. The confinement increase 39% as the eccentricity rises from 0 to 0.45, whereas load carried by RC core increases about 10%.



(a) Concentric Load



(b) 15 mm eccentric load

Figure 5.20 Maximum Concrete stresses at ultimate load for the column with different eccentricities

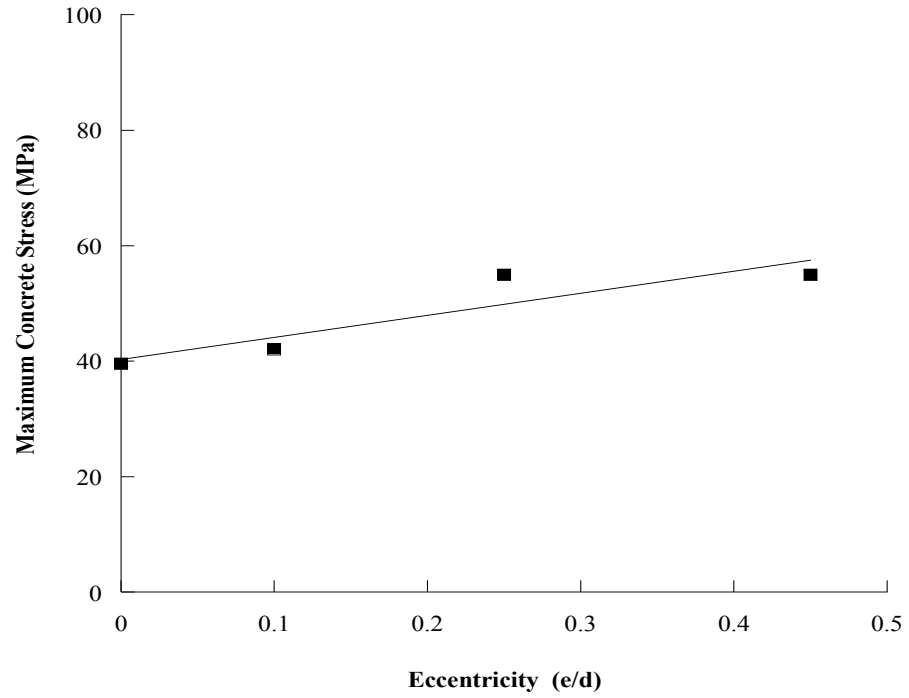


Figure 5.21 Confined concrete stress of jacketed RC columns at ultimate capacity

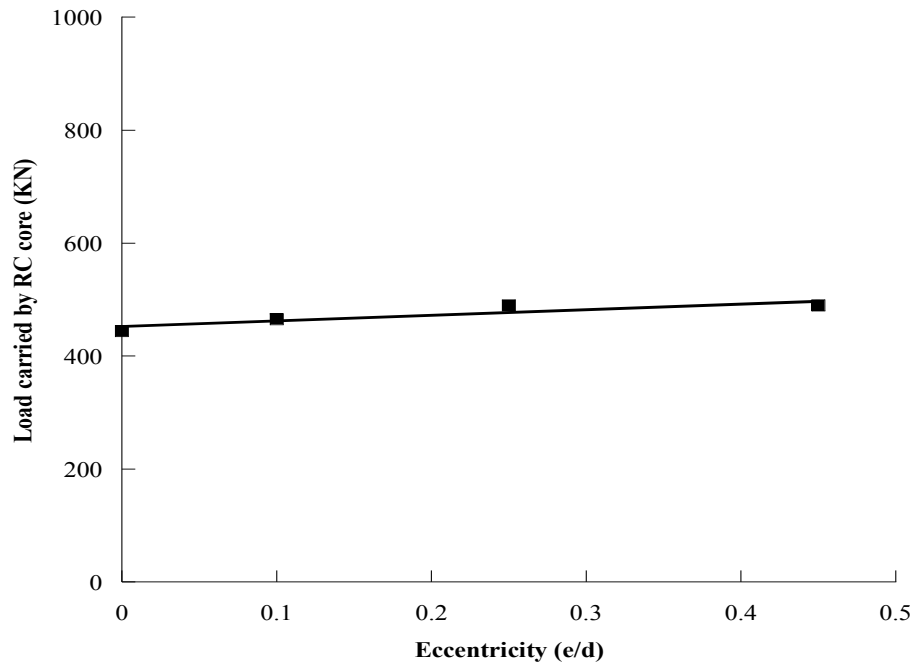
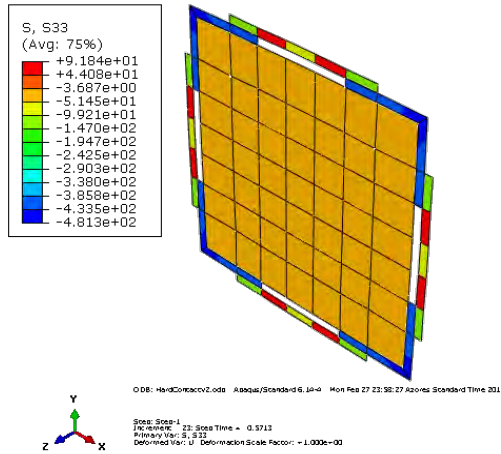


Figure 5.22 Load carried by RC core of jacketed columns at ultimate capacity

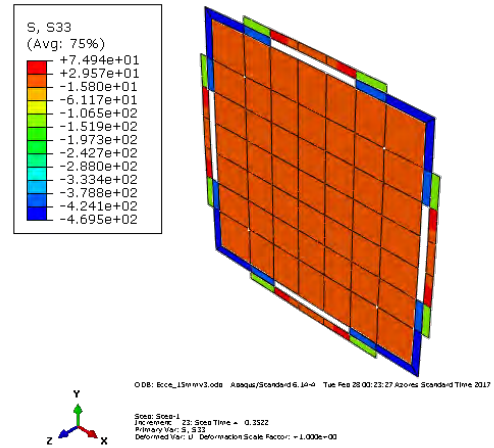
From the finite element analysis, it was found that for steel jacketed RC column the concrete confinement increases about 231% in case of concentric load compared to un-strengthened RC column. On the other hand, for the jacketed RC column loaded with an eccentricity to column width ratio 0.45 the enhancement is about 293%, which reflect the higher efficiency of steel cage under eccentric loading.

5.3.4 Mid-height displacement of angle

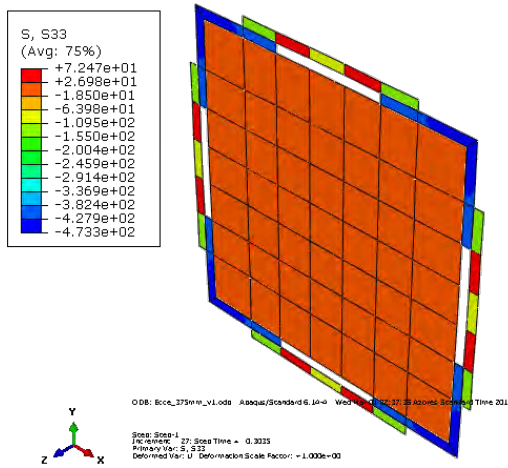
The impact on the mid height displacement of jacketed RC columns has been studied since maximum column displacement occurs at the mid level of column. Generally mid height displacement increases with the increase of eccentricity due to the stress concentration. To verify this phenomenon stresses of compression angles for all jacketed RC columns at a specific applied displacement i.e. 10 mm have been acquired from finite element analysis. This displacement is the point after that jacketed RC column yields under concentric load. At this displacement, compression side steel angles of concentrically loaded jacketed RC column have to take average stress of 433 MPa, which is less than yield stress. For the same axial displacement, eccentrically loaded jacketed RC columns have to take more compressive stress which is about 470 MPa. The stress contours are shown in Figure 5.23. Under eccentric loading this stress concentration causes early yielding of angles, which leads to a lower axial capacity and more mid-height displacement. This finding is also reported by Elsamny *et al.* (2013). Figure 5.24 shows the effect of eccentricity on the mid-height displacement. It is obvious from this figure that mid-height displacement increases about 16 percent as the eccentricity to column width ratio rises from 0 to 0.45.



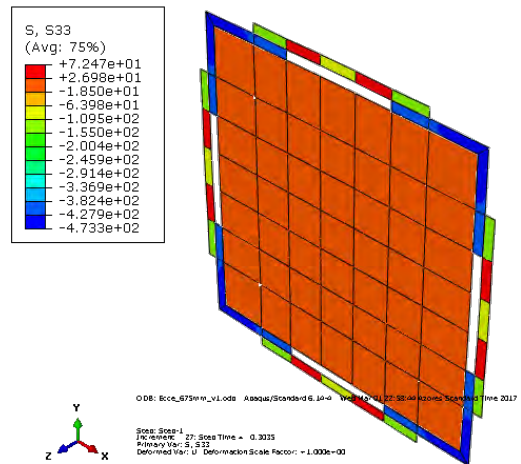
(a) Concentric load



(b) 15mm load eccentricity



(c) 37.5mm load eccentricity



(d) 67.5mm load eccentricity

Figure 5.23 Stress distributions at mid-height section for column having different load eccentricities

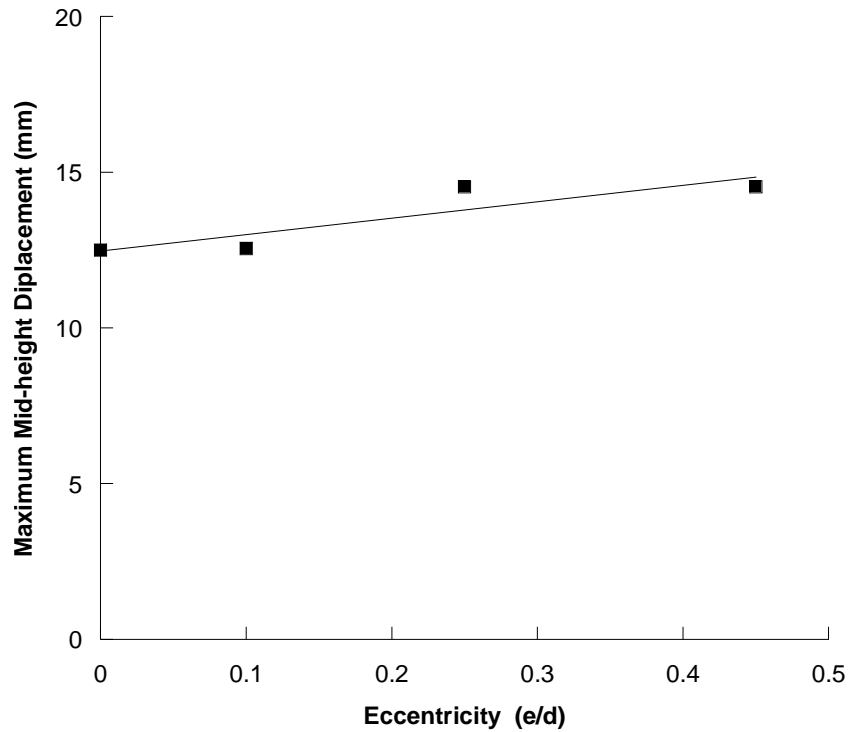


Figure 5.24 Effect of eccentricity on the mid height displacement

5.4 Performance of Analytical Models

5.4.1 Compressive capacity prediction models

In literature, it has been found that most of the researchers worked on the concentric jacketed RC columns and introduced some analytical models. Figure 5.25 shows a comparative scenario of different analytical models to predict the ultimate capacity of steel jacketed RC column (CA2). Experimental capacity of this column was found to be 1235 KN under direct concentric loading. Predicted capacities are presented in Table 5.4.

Capacity prediction models prescribed by Tarabia and Albakry (2014), Campione (2013) and Euro Code (1994) show a good agreement with the test result. Euro code (1994) only considers the composite action of RC core and steel cage, while other two models consider confinement due to steel caging also. These models somehow ignore the premature local buckling phenomenon which coincides with the condition of this test column. Rest of the models show little deviation from the test results. Khalifa and Al-Tersawy (2014) predicted

the capacity considering composite action and local buckling of steel elements. The predicted ultimate capacity is higher than the test result, which indicates an unsafe prediction.

Calderon *et al.* (2009) and Campione (2012) both prescribed analytical models considering yield of angles-strips separately. Both models give safe prediction with some deviation. These models predict higher capacity in case of strip yielding than angle yielding. It indicates the importance of the good bonding between angle and strips. If welding of steel angle and strip has enough strength to avoid premature joint failure, the capacity of steel jacketed column will increase in a large amount. These prediction models indicate that if strips yield, an increase of theoretical capacity is at least 27% for this particular test column.

So, it can be concluded that models considering composite action as well as confinement are appropriate for the directly loaded steel angle and strip jacketed short RC column, where premature local buckling in elastic range may not occur.

Table 5.4: Predicted capacities from different analytical models

References	Failure mode	Ultimate Capacity (KN)	Difference between different failure modes (%)
Khalifa and Al-Tersawy (2014)	-	1531	-
Tarabia and Albakry (2014)	-	1244	-
Campione (2013)	-	1180	-
Euro Code (1994)	-	1217	-
Campione (2012)	Angle yield	802	27
	Strip yield	1025	
Calderon <i>et al.</i> (2009)	Angle yield	401	35
	Strip yield	545	

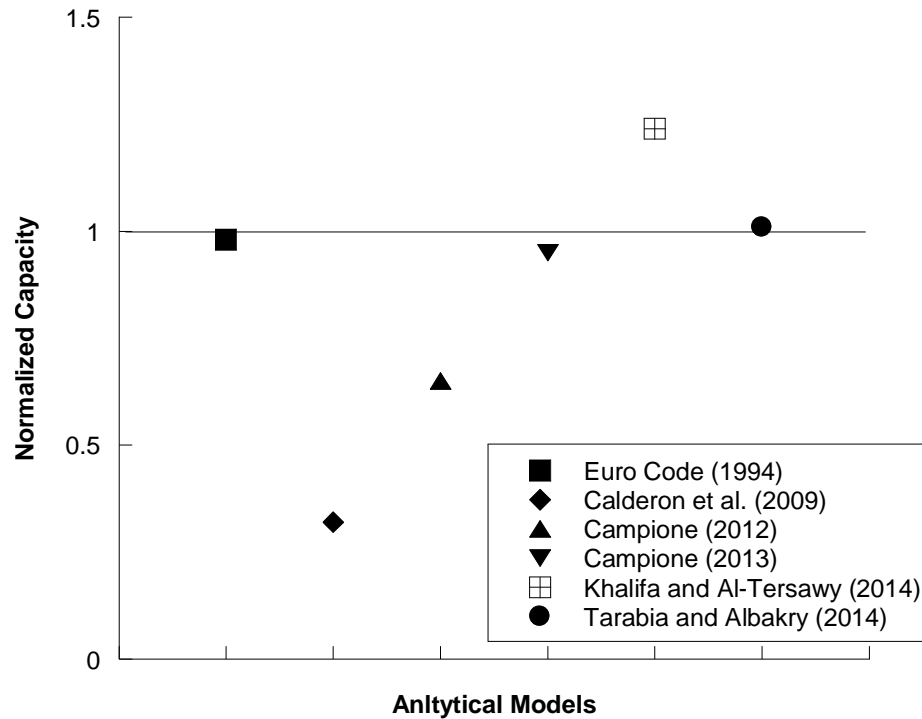


Figure 5.25 Normalized ultimate load capacities from different analytical models

5.4.2 Failure envelope prediction model

Campione (2013) proposed a simplified analytical model for moment and axial load domain for steel angle and strip jacketed RC columns. The analytical derivation is made for axial load and flexure assuming the equivalent stress-block parameters for internal forces. It also considers the confinement effects induced in the concrete core by external cages. This model considers load and moment under pure axial load, flexure and the case of balanced failure.

Figure 5.26 shows the predicted failure envelope as well as the experimental and FEM results. Experimental load-moment capacities of all steel jacketed RC columns, under both concentric and eccentric load, fall outside of the prescribed analytical failure envelope. It indicates safe prediction of the analytical model. On the other hand, finite element models predict slightly higher capacity than experimental capacity.

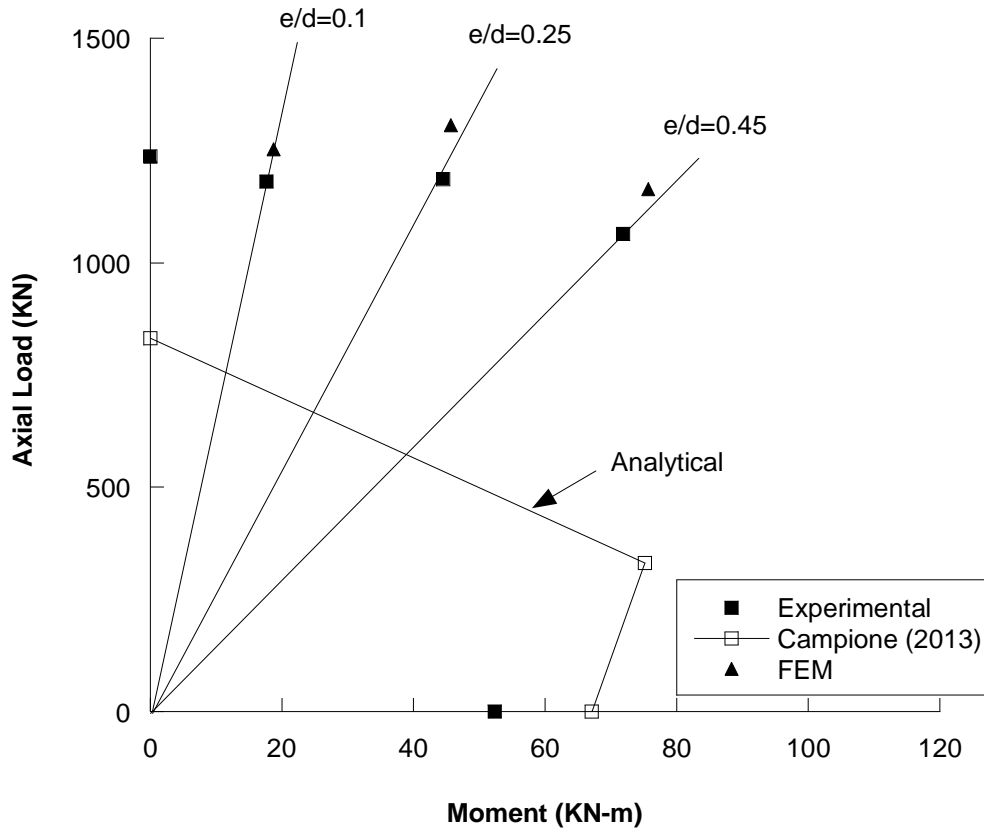


Figure 5.26 Analytical Interaction Diagram of jacketed RC column

Table 5.5 presents the interpolated load-moment capacities, computed using Figure 5.26, of steel jacketed RC columns by analytical model along with experimental and FEM capacities under various load eccentricities. The average of the ratio of FEM and analytical model's ultimate capacities to experimental capacities is 0.94 and 1.67 respectively. It indicates that analytical model gives more conservative prediction than FEM. Analytical model proposed by Campione (2013) underestimates the capacity of jacketed RC columns enormously. So, from this study this can be concluded that load-moment interaction diagram for eccentrically loaded jacketed RC columns can be achieved by using FEM or analytical model.

Table: 5.5: Axial and moment capacity of jacketed column

Eccentricity	Experimental		FEM		Analytical*		P_{exp}/P_{fem}	P_{exp}/P_{ana}
	Load (KN)	Moment (KN-m)	Load (KN)	Moment (KN-m)	Load (KN)	Moment (KN-m)		
0	1235	0	1235	0	830	0	1.00	1.48
0.10	1180	18	1250	19	750	12	0.94	1.57
0.25	1185	45	1305	46	675	25	0.91	1.76
0.45	1065	72	1165	76	575	39	0.91	1.85
Mean							0.94	1.67
Standard Deviation							0.04	0.17

* Analytical values are obtained by linear interpolation

5.5 Summary

An experimental study along with finite element modeling has been done to investigate the behavior of the steel angle and strip jacketed RC columns under different load eccentricities. In this study, variance parameter is the load eccentricity of jacketed RC columns. Eccentricity reduces the ultimate load capacity of steel angle and strip jacketed RC columns. Under eccentric loads jacketed RC columns show relatively more ductile failure as compared to the concentrically loaded column. This is due to the early activation of concrete confinement. Though eccentricity is not preferred due to reduction of axial capacity, however under eccentric loads steel angle and strip jacketing method works well. Finite element models can predict the ultimate load capacity of the steel angle and strip jacketed RC columns accurately with an experimental to finite element ultimate capacity ratio of 0.94. For concentrically loaded steel jacketed RC column enhancement of concrete confinement is about 231%. On the other hand, for eccentricity to column width ratio of 0.45 this enhancement has been found to be 293%. Existing analytical model (Campione, 2013) for load moment interaction diagram, based on strain compatibility, can safely be used

to predict the load-moment capacity of steel jacketed RC columns. However, it highly underestimates the actual capacity of strengthened RC column. Axial capacity prediction models show good agreement with experimental results. To choose the appropriate model, emphasis should be given on exact loading process (i.e. direct or indirect) and expected failure mode.

CHAPTER 6

CONCLUSIONS AND RECOMMENDATIONS

6.1 General

In this study, an experimental program including un-strengthened and strengthened RC columns has been designed to investigate the behaviour of steel angle and strip jacketed RC columns under eccentric loads. The RC columns have 150 mm square cross section, 1.4% longitudinal reinforcement and a slenderness ratio of 10. RC columns have been constructed with very low concrete strength (10 MPa) intentionally. Strengthening of RC columns have been done using steel angles (8.4% of concrete cross section) and strips. Test columns have been loaded using steel cap and steel plate at top and bottom respectively. Top steel caps have been designed to apply eccentric loads. Load eccentricity has been taken as the variable since deficiency of researches has been found on the load eccentricity in literature, which has profound influences on the behavior of jacketed RC columns. Load-deflection behaviour, ultimate capacity and displacement ductility of tested steel jacketed RC columns have been compared with a RC column without jacketing.

Nonlinear 3D finite element models have been developed in Finite Element platform (ABAQUS/Standard) to simulate the experimental works. Numerical simulation has been conducted by considering damage plasticity model of concrete and bi-linear stress strain curve of steel materials. Performance of the numerical model was checked with experimental results in terms of ultimate load capacities and failure modes. As numerical models show fair agreement with the experimental results. Finally, load-moment interaction diagram has been developed from experimental results and compared with available analytical model as well as finite element analysis conducted in this study.

6.2 Conclusions

The following conclusions may be drawn within the limited scope of this study.

- From the experimental investigations on steel jacketed short RC columns (150x150 mm) with 1.4% longitudinal and 8.4% strengthening steel, it has been found that under concentric loading steel angle and strip jacketed RC column shows an increase in ultimate capacity of 240% as compared to an un-strengthen RC column. On the other hand, this increase of ultimate capacity varies from 330% to 850% as the eccentricity to column width ratio rises from 0 to 0.45. This enhancement can be attributed to the early activation of the confinement. The concrete confinement increases by 39% as the eccentricity rises from 0 to 0.45. However, further experimental studies on full scale specimens are required to conclude this behavior firmly.
- The finite element model developed in this study is capable of predicting the load-moment failure surface with good accuracy. The average value of experimental to numerical ultimate load capacity ration was obtained 0.94 with a standard deviation of 0.04.
- Steel jacketing retrofitting method not only improves the ultimate capacity of the RC column but also significantly increases the axial deformation at the ultimate point. This results in improved ductility of the strengthen column. In general, failure of the jacketed RC column occurred in un-strengthened part (i.e. in between strips) by inelastic buckling of compression side steel angles after reaching yield stress. This was followed by crushing of concrete. In columns with higher load eccentricities significant amount of global buckling was observed.
- Presence of eccentricity reduces the ultimate load capacity of steel angle and strip jacketed RC columns. The ultimate capacity of steel jacketed RC columns reduces by 15% for an increase of load eccentricity to column width (e/d) ratio from 0 to 0.45.

- Under eccentric loads jacketed RC columns show relatively more ductile failure as compared to the concentrically loaded column. This is due to the early activation of concrete confinement. Though eccentricity is not preferred due to reduction of axial capacity, but under eccentric loads steel angle and strip jacketing method works well.
- Under lower eccentricity ($e/d = 0.1$) strengthened RC column shows 4.3 times higher axial capacity than the un-strengthened RC column subjected to same levels load eccentricity, whereas for the higher eccentricity ($e/d = 0.45$) the capacity of strengthened RC column is 9.5 times higher than corresponding un-strengthened RC column.
- Load-moment interaction curve computed using the analytical model proposed by Campione (2013) can be a handy solution for designer to check the adequacy of jacketed RC columns. The average ratio of experimental to analytical ultimate load capacity was obtained 1.67, which indicates highly conservative prediction of the model with a standard deviation of 0.17. The analytical model proposed by Campione (2013) can be used to predict the load and moment capacities of steel jacketed RC columns with a high level of safety margin.

6.3 Recommendations for Future Work

This study assumed the undamaged condition of RC column before strengthening. In real filed strengthening has to be done with damaged or deteriorated column. Therefore, load application before strengthening is recommended for the future works.

The lateral deformation due to the application of gradual axial load increases the instantaneous moment. This phenomenon is known as P- Δ effect, which is ignored in this study. Therefore, inclusion of P- Δ effect is recommended.

This study only investigate the effect of eccentricity keeping jacketing configuration same. Future research may incorporate the variation of angle and strip configuration.

REFERENCES

Abdel-Hay, A. S., and Fawzy, Y. A. G. (2015). "Behavior of partially defected RC columns strengthened using steel jackets." *HBRC Journal*, 11(2), 194-200.

Adam, J. M., Ivorra, S., Pallarés, F. J., Giménez, E., and Calderón, P. A. (2009). "Axially loaded RC columns strengthened by steel caging: Finite element modelling." *Construction and Building Materials*, 23(6), 2265-2276.

Almusallam, T. H., and Alsayed, S. H. (1995). "Stress-strain relationship of normal, high-strength and lightweight concrete." *Magazine of Concrete Research*, 47(170), 39-44.

Areemit, N., Faeksin, N., Niyom, P., and Phonsak, P. (2013). "Strengthening of deficient RC columns by steel angles and battens under axial load." In *Proceedings of the Thirteenth East Asia-Pacific Conference on Structural Engineering and Construction (EASEC-13)*.

Badalamenti, V., Campione, G., and Mangiavillano, M. L. (2009). "Simplified model for compressive behavior of concrete columns strengthened by steel angle and strip." *Journal of Engineering Mechanics*, 136(2), 230-238.

Belal, M. F., Mohamed, H. M., and Morad, S. A. (2015). "Behavior of reinforced concrete columns strengthened by steel jacket." *HBRC Journal*, 11(2), 201-212.

Braga, F., Gigliotti, R., and Laterza, M. (2006). "Analytical stress-strain relationship for concrete confined by steel stirrups and/or FRP jackets." *Journal of Structural Engineering*, 132(9), 1402-1416.

Calderón, P. A., Adam, J. M., Ivorra, S., Pallarés, F. J., and Giménez, E. (2009). "Design strength of axially loaded RC columns strengthened by steel caging." *Materials and Design*, 30(10), 4069-4080.

Campione, G. (2011). "RC columns strengthened with steel angles and battens: experimental results and design procedure." *Practice Periodical on Structural Design and Construction*, 18(1), 1-11.

Campione, G. (2013). "Simplified analytical model for RC columns externally strengthened with steel cages." *Journal of Civil Engineering and Science*, 2(4), 212-218.

Carreira, D. J., and Chu, K. H. (1985). "Stress strain relationship for plain concrete in compression." *ACI Journal*, 82(6), 796-804.

Delgado, P., Rodrigues, V., Rocha, P., Santos, M., Arêde, A., Pouca, N. V., and Delgado, R. (2005). "Seismic retrofitting of structural elements. An experimental characterization." *250th Anniversary of the 1755 Lisbon Earthquake*, Portugal.

Dolce, M., Masi, A., Cappa, T., Nigro, D., and Ferrini, M. (2003). "Experimental evaluation of effectiveness of local strengthening on columns of R/C existing structures." In *Proceedings of fib-symposium Concrete Structures in Earthquake Regions*, Athens, Greece.

Elsamny, M. K., Hussein, A. A., Nafie, A. M., and Abd-Elhamed, M. K. (2013). "Experimental study of eccentrically loaded columns strengthened using a steel jacketing technique." *International Journal of Civil, Architectural, Structural and Construction Engineering*, 7(12), 558-565.

European Committee for Standardization (CEN). (2003). "Design of structures for earthquake resistance. Part3: Strengthening and repair of buildings." *Eurocode 8*, CEN, Brussels, Belgium.

Garzón-Roca, J., Adam, J. M., Calderón, P. A., and Valente, I. B. (2012). “Finite element modeling of steel-caged RC columns subjected to axial force and bending moment.” *In Proceedings of the Eleventh International Conference on Computational Structures Technology*, Stirlingshire, Scotland.

Giménez, E., Adam, J. M., Ivorra, S., Moragues, J. J., and Calderón, P.A. (2009). “Full-scale testing of axially loaded RC columns strengthened by steel angle and strip.” *Advances in Structural Engineering*, 2(12), 169-81.

Giménez, E., Adam, J. M., Ivorra, S., and Calderón, P. A. (2009). “Influence of strips configuration on the behaviour of axially loaded RC columns strengthened by steel angle and strip.” *Materials and Design*, 30(10), 4103-4111.

Hibbitt, Karlsson and Sorensen, Inc. (HKS) (2013). *ABAQUS/ Standard User's Manual*, Version 6.3.

Khalifa, E. S., and Al-Tersawy, S. H. (2014). “Experimental and analytical behavior of strengthened reinforced concrete columns with steel angle and strip.” *International Journal of Advanced Structural Engineering (IJASE)*, 6(2), 1-14.

Li, J., Gong, J., and Wang, L. (2009). “Seismic behavior of corrosion-damaged reinforced concrete columns strengthened using combined carbon fiber-reinforced polymer and steel jacket.” *Construction and Building Materials*, 23(7), 2653-2663.

Lubliner, J., Oliver, J., Oller, S., and Onate, E. (1989). “A plastic-damage model for concrete.” *International Journal of solids and structures*, 25(3), 299-326.

Makki, R.F., and Nimmim, S.T. (2015). “Rehabilitation of structural columns by using steel angles.” *International Journal of Scientific and Engineering Research*, 1(6), 981-987.

Marzouk, H., and Chen, Z. W. (1995). “Fracture energy and tension properties of high-

strength concrete.” *Journal of Materials in Civil Engineering*, 7(2), 108-116.

Monti, G. (2003). “Seismic upgrade of reinforced concrete columns with FRP.” In *Seminar on: Seismic Retrofitting of the South Tower*, Tehran, Iran.

Nagaprasad, P., Sahoo, D. R., and Rai, D. C. (2009). “Seismic strengthening of RC columns using external steel cage.” *Earthquake Engineering and Structural Dynamics*, 38(14), 1563-1586.

Ong, K. C. G., and Kang, J. H. (2004). “Jacketing of preloaded steel columns.” *Journal of Constructional Steel Research*, 60(1), 109-124.

Shin, M., and Andrawes, B. (2010). “Experimental investigation of actively confined concrete using shape memory alloys.” *Engineering Structures*, 32(3), 656-664.

Tarabia, A. M., and Albakry, H. F. (2014). “Strengthening of RC columns by steel angle and strip.” *Alexandria Engineering Journal*, 53(3), 615-626.

Taranu, N., Cozmanciuc, C. I., and Oltean, R. (2011). “Experimental study of reinforced concrete columns confined with composite membranes.” *Buletinul Institutului Politehnic din Iasi. Sectia Constructii, Arhitectura*, 57(3), 33-45.

APPENDIX

Table A.1 Details of samples and results with different number of strips and eccentricity

Reference	Model & Cross Section	Material Strength f_{cu}	Corner Angle ($L_1 \times L_1 \times t_1$)	Strip Size ($L_2 \times t_2$)	Strip Spacing S	No. of strips	Angle to Specimen Head Connection	Grout Material	Eccentricity	Axial Shortening	Ultimate Load Capacity	Increase in Load Capacity
									(e/h)	(mm)	(KN)	(%)
	(mm x mm)	(N/mm ²)	(mm)	(mm)	(mm)			(%)	(mm)	(KN)	(%)	
Tarabia and Albakry (2014)	SC1 (150 x 150)	57.80	50 x 50 x 4.5	-	170	-	Con.	Cement	0	0.99	2570	74
	SC2 (150 x 150)	47.50	30 x 30 x 3	-	170	-	Con.	Cement	0	1.06	2190	108
	SCN1 (150 x 150)	57.80	50 x 50 x 4.5	-	170	-	Not Con.	Cement	0	1.00	1990	35
	SCN2 (150 x 150)	47.50	30 x 30 x 3	-	170	-	Not Con.	Cement	0	1.17	2000	90
	SE1 (150 x 150)	57.80	50 x 50 x 4.5	-	170	-	Con.	Epoxy	0	1.64	2600	76
	SE2 (150 x 150)	47.50	30 x 30 x 3	-	170	-	Con.	Epoxy	0	1.04	2150	99
	SCW1 (150 x 150)	57.80	50x50x4.5	-	260	-	Con.	Cement	0	0.83	2310	57
	SCW2 (150 x 150)	47.50	30x30x3	-	260	-	Con.	Cement	0	0.93	2050	95
	C1 T3 (120 x 120)	15	20 x 20 x 2	20 x 2	490	3	Con.	Epoxy	8.3	-	390	-
	C2 T5 (120 x 120)	15	20 x 20 x 2	20 x 2	245	5	Con.	Epoxy	8.3	-	360	-
Elsamny <i>et al.</i> (2013)	C3 T7 (120 x 120)	15	20 x 20 x 2	20 x 2	164	7	Con.	Epoxy	8.3	-	340	-
	C4 T3 (120 x 120)	15	20 x 20 x 2	20 x 2	490	3	Con.	Epoxy	16.6	-	290	-
	C5 T5 (120 x 120)	15	20 x 20 x 2	20 x 2	245	5	Con.	Epoxy	16.6	-	250	-
	C6 T7 (120 x 120)	15	20 x 20 x 2	20 x 2	164	7	Con.	Epoxy	16.6	-	250	-
	C7 T3 (120 x 120)	15	20 x 20 x 2	20 x 2	490	3	Con.	Epoxy	25	-	255	-
	C8 T5 (120 x 120)	15	20 x 20 x 2	20 x 2	245	5	Con.	Epoxy	25	-	210	-
	C9 T7 (120 x 120)	15	20 x 20 x 2	20 x 2	164	7	Con.	Epoxy	25	-	210	-
	C10 T3 (120 x 120)	15	20 x 20 x 2	20 x 2	490	3	Con.	Epoxy	33.3	-	175	-

Reference	Model & Cross Section	Material Strength f_{cu}	Corner Angle ($L_1 \times L_1 \times t_f$)	Strip Size ($L_2 \times t_f$)	Strip Spacing S	No. of strips	Angle to Specimen Head Connection	Grout Material	Eccentricity (e/b)	Axial Shortening	Ultimate Load Capacity	Increase in Load Capacity
	(mm x mm)	(N/mm ²)	(mm)	(mm)	(mm)				(%)	(mm)	(KN)	(%)
Khalifa and Tersawy (2014)	C11 T5 (120 x 120)	15	20 x 20 x 2	20 x 2	245	5	Con.	Epoxy	33.3	-	175	-
	C12 T7 (120 x 120)	15	20 x 20 x 2	20 x 2	164	7	Con.	Epoxy	33.3	-	175	-
	C20A1X1 (120 x 120)	30	10 x 10 x 2	-	490	3	Con.	Epoxy	25	-	-	19
	C21A2X2 (120 x 120)	30	20 x 20 x 2	-	490	3	Con.	Epoxy	25	-	-	42
	C22A4X4 (120 x 120)	30	40 x 40 x 2	-	490	3	Con.	Epoxy	25	-	-	58
	CS1 (150 x 150)	32.8	40 x 40 x 5	50 x 5	237.5	5	Con.	-	0	1.85	676.2	36.5
	CS2 (150 x 150)	32.8	40 x 40 x 6	50 x 6	237.5	5	Con.	-	0	2.35	789.5	59.3
Makki, and Nimmim (2015)	CS3 (150 x 150)	32.8	50 x 50 x 5	50 x 5	237.5	5	Con.	-	0	2.04	730.8	47.5
	CS4 (150 x 150)	32.8	50 x 50 x 6	50 x 6	237.5	5	Con.	-	0	2.67	821.3	65.8
	B1 (120 x 120)	25	25 x 25 x 3	25 x 3	-	-	Con.	-	0	-	760	83.1
	B2 (120 x 120)	25	32 x 32 x 5	25 x 3	-	-	Con.	-	0	-	885	113.3
Campione (2011)	B3 (120 x 120)	25	40 x 40 x 5	25 x 3	-	-	Con.	-	0	-	920	121.7
	2 (215 x 215)	10	30 x 30 x 3	30 x 3	600	2	Not Con.	Epoxy	0	3.50	663	31.5
	3 (215 x 215)	10	30 x 30 x 3	30 x 3	300	3	Not Con.	Epoxy	0	3.63	757	50.2
	4 (215 x 215)	10	30 x 30 x 3	30 x 3	200	4	Not Con.	Epoxy	0	4.35	864	71.1

Con. = Connected to specimen head
Not con. = Not connected to specimen head

Table A.2 Details of samples and results with different strip configuration

Reference	Model & Cross Section	Material Strength f_{cu}	Corner Angle ($L_1 \times L_1 \times t_f$)	Strip Size ($L_2 \times t_f$)	Strip Spacing S	Strip Configuration	Grout Material	Loading State	Angle to Specimen Head Connection	Ultimate Load Capacity P_{ult}	Increase in Load Capacity
	(mm x mm)	(N/mm ²)	(mm)	(mm)	(mm)					(KN)	(%)
Giménez <i>et al.</i> (2009)	AD (300x300)	15.4	80 x 80 x 8	160 x 8	575	A	Cement	Unloaded	Not. Con.	2652	80
	BD (300x300)	10.2	80 x 80 x 8	160 x 8	575	A	Cement	Unloaded	Con.	2111	75
	MEAD (300x300)	8.3	80 x 80 x 8	160 x 8	575	A	Epoxy	Unloaded	Not. Con.	1855	67
	MEBD (300x300)	8.3	80 x 80 x 8	160 x 8	575	A	Epoxy	Unloaded	Con.	2040	81
	AC (300x300)	12.3	80 x 80 x 8	160 x 8	575	A	Cement	Loaded	Not. Con.	2300	75
	BC (300x300)	14.2	80 x 80 x 8	160 x 8	575	A	Cement	Loaded	Con.	2261	60
Giménez <i>et al.</i> (2009)	PAD (300x300)	8.3	80 x 80 x 8	160 x 8	575	B	Cement	Unloaded	Not. Con.	2432	109
	PBD (300x300)	8.3	80 x 80 x 8	160 x 8	575	B	Cement	Unloaded	Con.	2648	125
	PAC (300x300)	8.3	80 x 80 x 8	160 x 8	575	B	Cement	Loaded	Not. Con.	2256	97
	PBC (300x300)	8.3	80 x 80 x 8	160 x 8	575	B	Cement	Loaded	Con.	2524	117
Areemit <i>et al.</i> (2013)	A (200x200)	9.1	40 x 40 x 4	50 x 4	150	A	Epoxy	-	Not Con.	1035	70.5
	B (200x200)	9.1	40 x 40 x 4	50 x 4	150	B	Epoxy	-	Not Con.	1066	75.6
	C (200x200)	9.1	40 x 40 x 4	25 x 4	75	A	Epoxy	-	Not Con.	1031	69.9

Strip configuration:

A = Strips are equally distributed

B = Strips are equally distributed with additional strips at ends.